PIERRE AUGER OBSERVATORY

Search for ultra-high-energy cosmic ray counterparts

Gašper Kukec Mezek

University of Nova Gorica[1]
for the Pierre Auger Collaboration[2]

Multimessenger data analysis in the era of CTA (Sexten, June 26th 2019)

[1]University of Nova Gorica, Center for Astrophysics and Cosmology, Vipavska 11c, 5270 Ajdovščina, Slovenia
[2]Observatorio Pierre Auger, Av. San Martín Norte 304, 5613 Malargüe, Argentina
E-mail: auger_spokespersons@fnal.gov

Outline

1. Cosmic rays (CR) and extensive air showers (EAS)
2. Pierre Auger Observatory
3. Anisotropy studies
   - Large-scale anisotropy (E > 4 EeV)
   - Intermediate-scale anisotropy (E > 20 EeV)
4. Multimessenger studies
   - Search for neutrinos
     - Diffuse neutrino search
     - Point source neutrino search
   - Search for photons
     - Diffuse photon search
     - Point source photon search

Cosmic rays and extensive air showers

Cosmic rays (CR): Charged particles arriving to Earth from extraterrestrial sources

Ultra-high-energy cosmic rays (UHECR): CR with energies above ~10^{18} eV

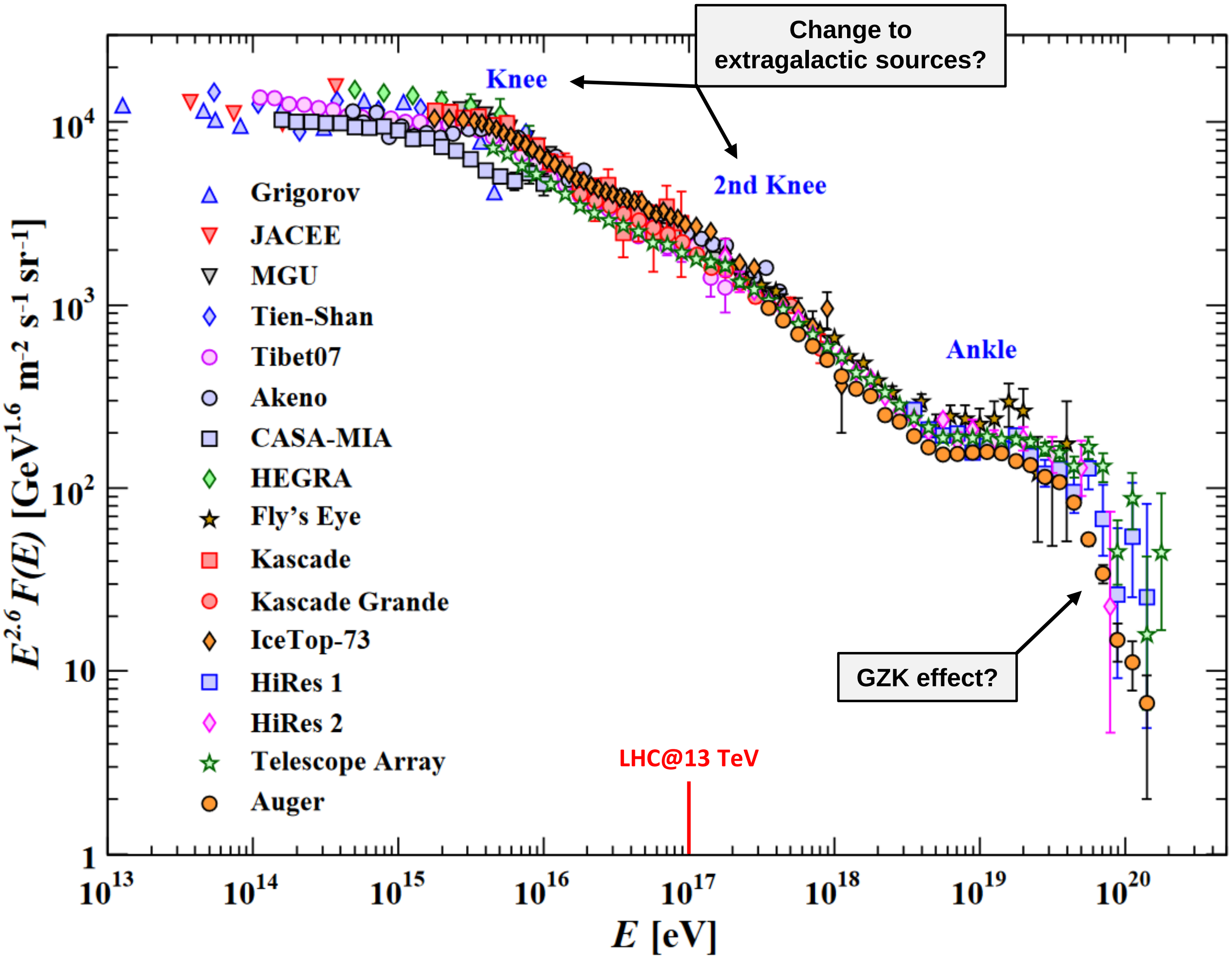

Cosmic rays and extensive air showers

Extensive air showers (EAS): Cascade of secondary particles after interaction of UHECR and atmospheric nuclei

EAS consists of the EM part (electrons, positrons, photons), hadronic part (hadrons, mesons) and weakly interacting shower remnants (muons, neutrinos)

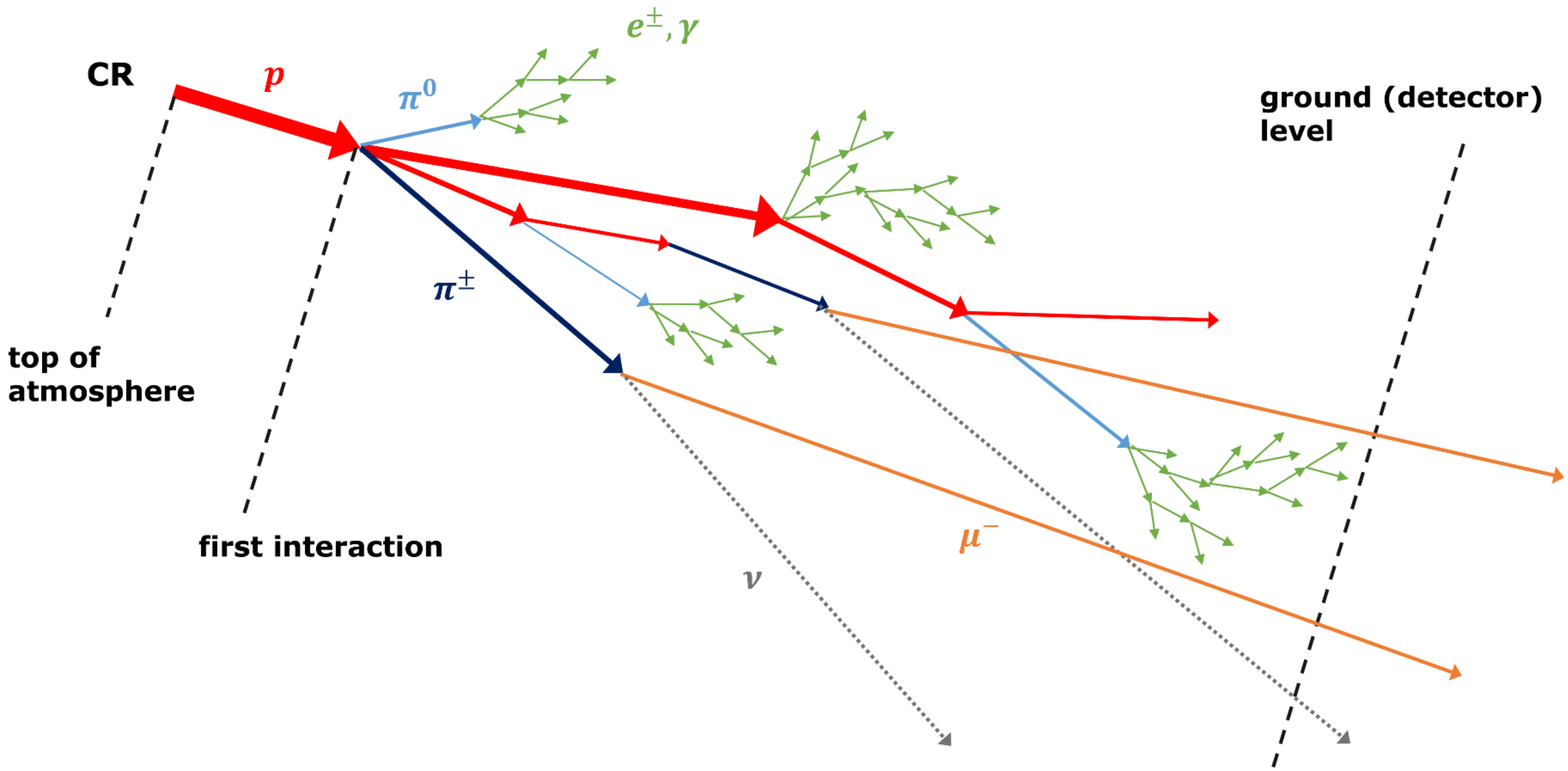

Cosmic rays and extensive air showers

Extensive air showers (EAS): Cascade of secondary particles after interaction of UHECR and atmospheric nuclei

EAS consists of the EM part (electrons, positrons, photons), hadronic part (hadrons, mesons) and weakly interacting shower remnants (muons, neutrinos)

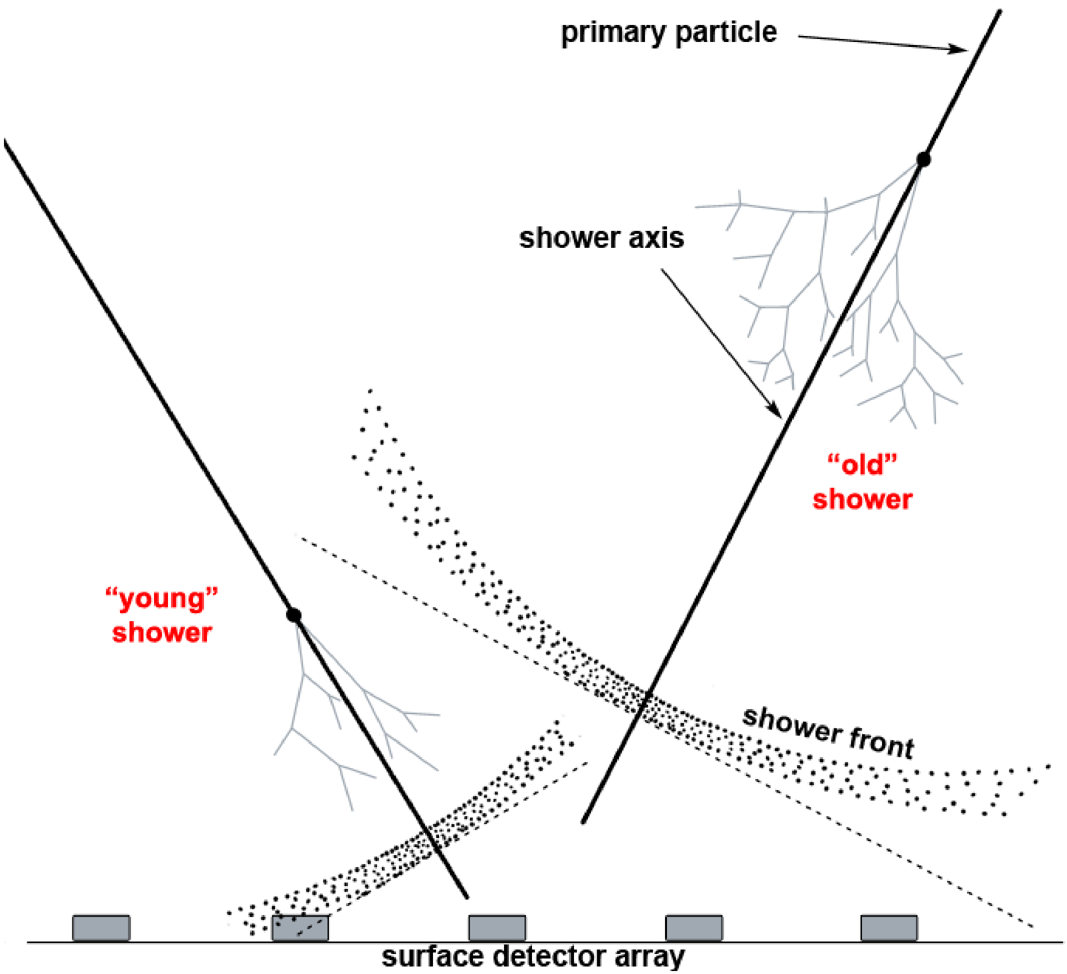

Primary particle type determines evolution of the EAS:

Larger interaction cross section → EAS develops earlier in the atmosphere

Smaller interaction cross section → EAS develops deeper in the atmosphere

The younger the shower, the larger the EM content at ground level compared to muonic content

Pierre Auger Observatory

SD: 1600 water-Cherenkov stations, 1500 m separation, 3000 km^2 area

FD: 24 fluorescence telescopes at 4 locations

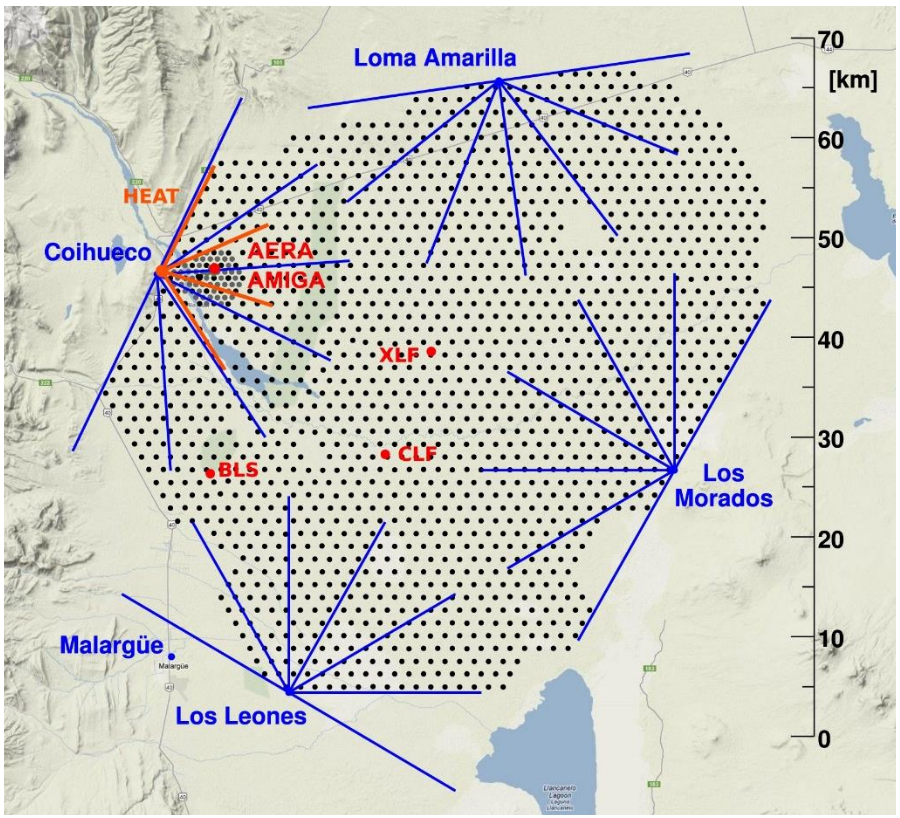

Low energy upgrade

SD (750 m): 61 water-Cherenkov stations, 750 m separation, 23.5 km^2 area

FD (HEAT): 3 fluorescence telescopes close to Coihueco FD location

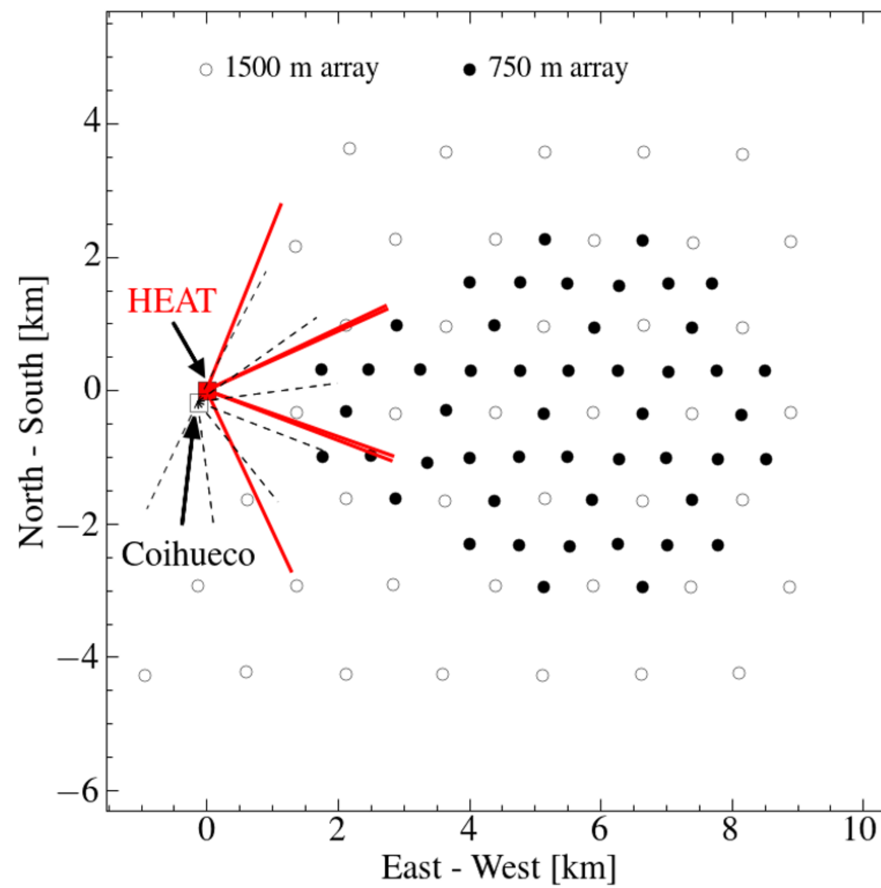

SD water-Cherenkov stations

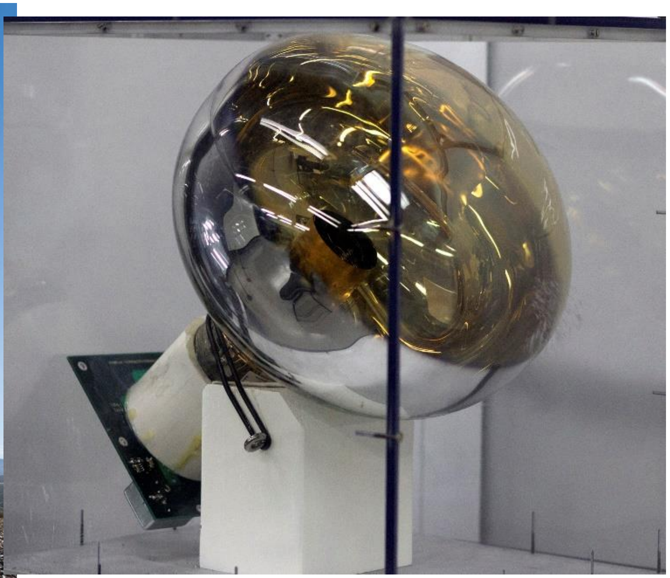

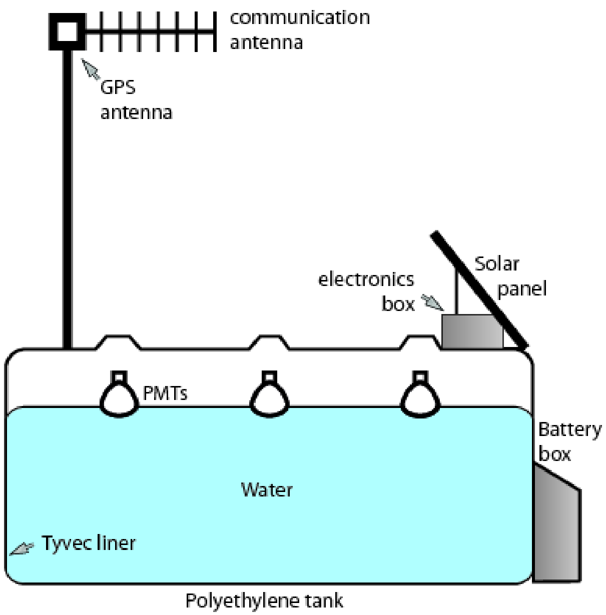

Each station filled with 12 tonnes of deionized water

Passing charged particles produce Cherenkov light, detected by 3 PMTs

Operational nearly 100% of the time

750 m array reduces lower energy limit from $10^{18.5}$ to $10^{17.2}$ eV

Fluorescence detector telescopes

Standard-FD

FOV 0° to 30° elevation
Low energy limit: $10^{17.8}$ eV

HEAT (in up position)

FOV 30° to 60° elevation
Energy range: $10^{17.2}$ eV – $10^{18.1}$ eV

Measurement of fluorescent light (N deexcitation, 300-450 nm)

440 PMT camera (1.5° per pixel)

FD measurements operational ~15% of the time (clear nights, low moon fraction)

Anisotropy studies

Anisotropy: Gain information on sources from arrival directions of UHECR

Estimating dipole structure of arrival directions (galactic versus extragalactic sources)

Correlation of arrival directions with catalogs of astrophysical sources

Large scale anisotropy → Low energies
Small scale anisotropy → High energies

Main difficulties come from the unclear mass composition and magnetic field strength

$$\Delta\alpha = \frac{Z\ e\ c}{E} \int_0^L B(x) \sin(\varphi(x))\, dx$$

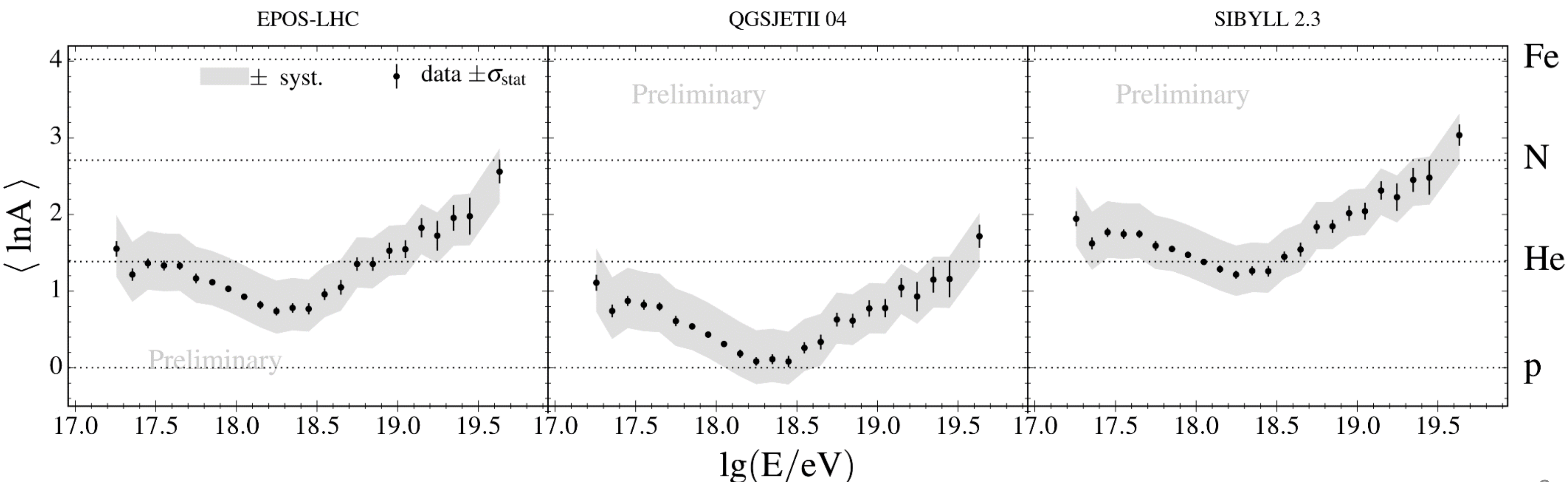

Large-scale anisotropy

Large-scale anisotropy: Search for modulation of arrival directions above 4 EeV

Auger data between January 1st 2004 and August 31st 2016, exposure 76,800 km^2 sr yr

Perform a Fourier analysis on RA (α) and azimuth (ϕ) → gain information on structure and estimate UHECR flux excess

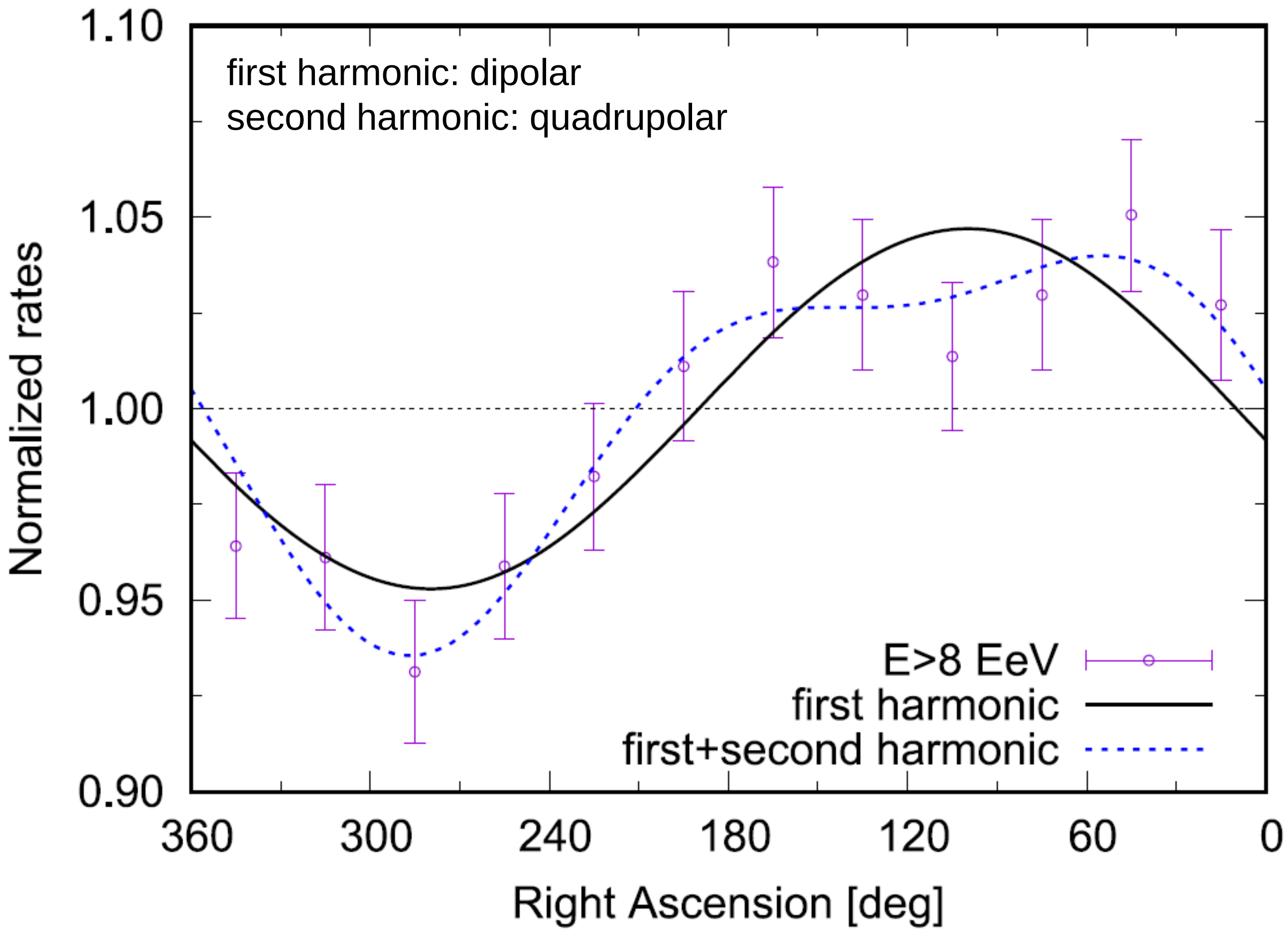

Cosmic ray flux maps

4 EeV ≤ E < 8 EeV:
Excess from southern direction

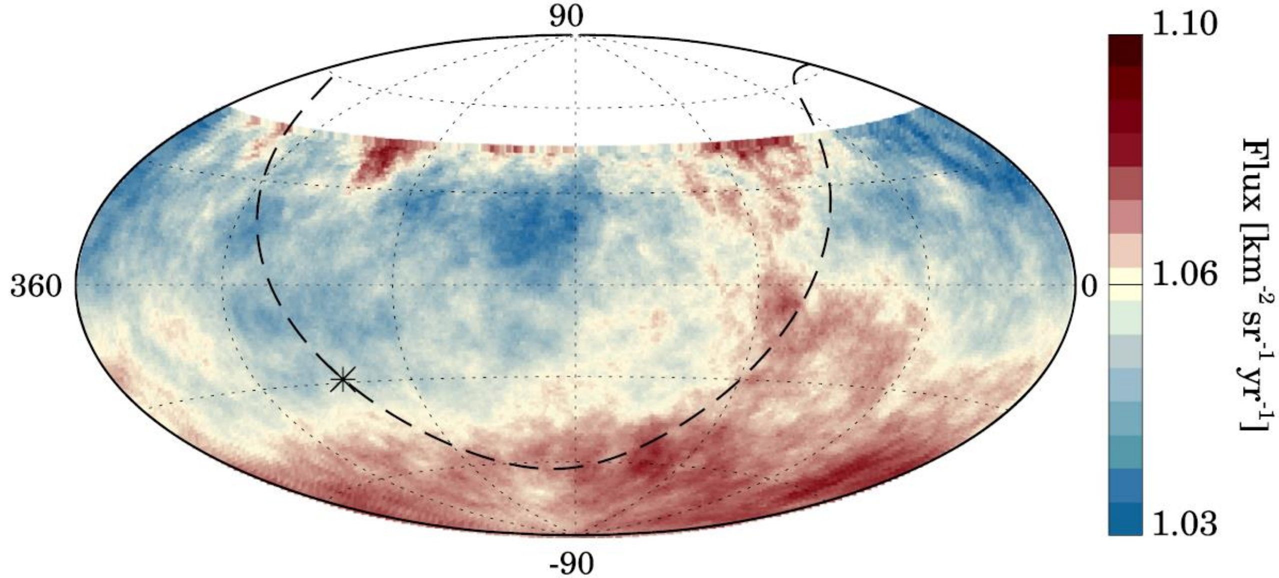

E ≥ 8 EeV:
Excess at RA ~ 100°, deficit in opposite direction

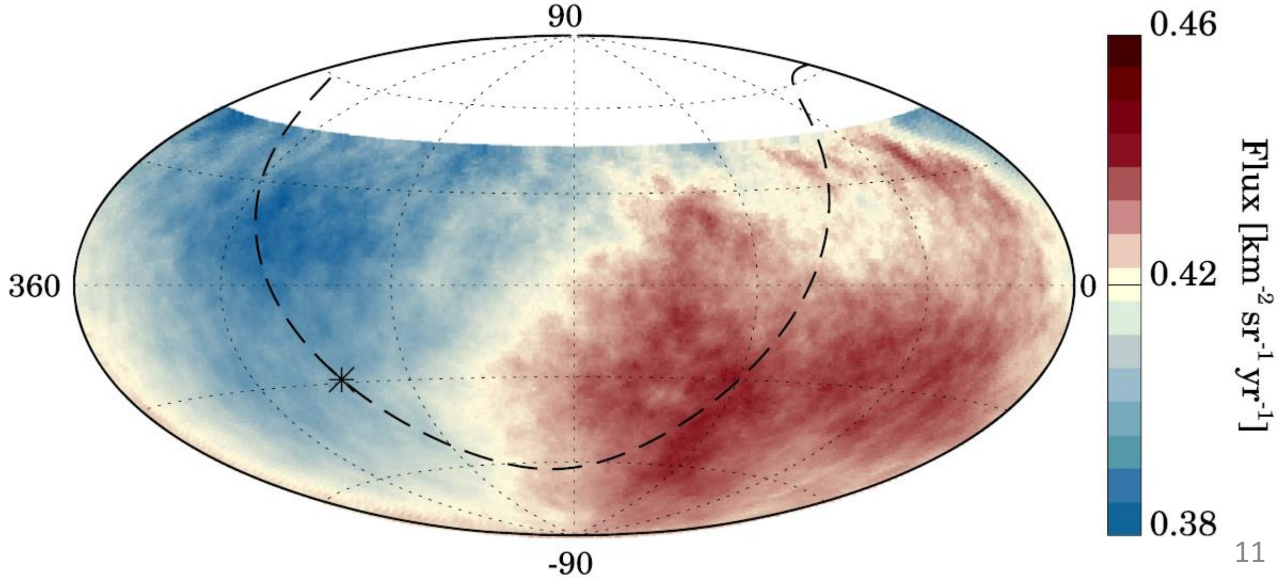

Maps are in equatorial coordinates

Dipolar structure

Highest energy bin split into three bins in order to get the dipolar amplitude dependence

Dipole $\boldsymbol{d}$ is calculated from RA and azimuth

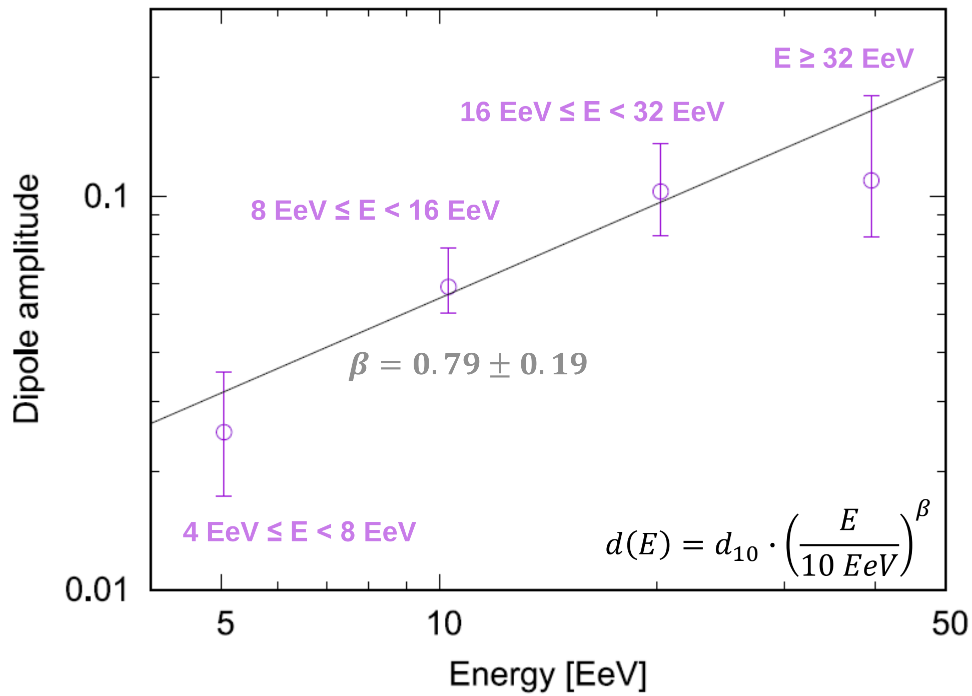

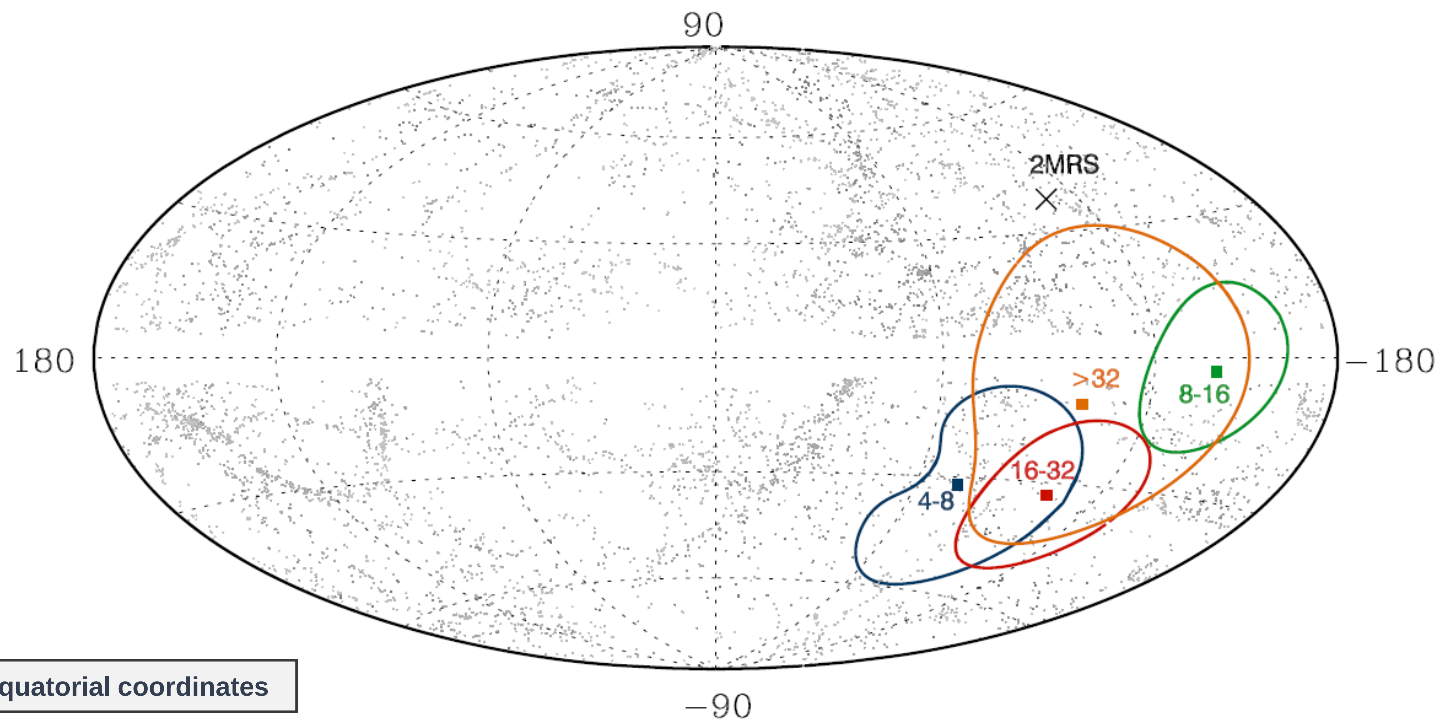

Maps are in equatorial coordinates

Cosmic ray excess maps

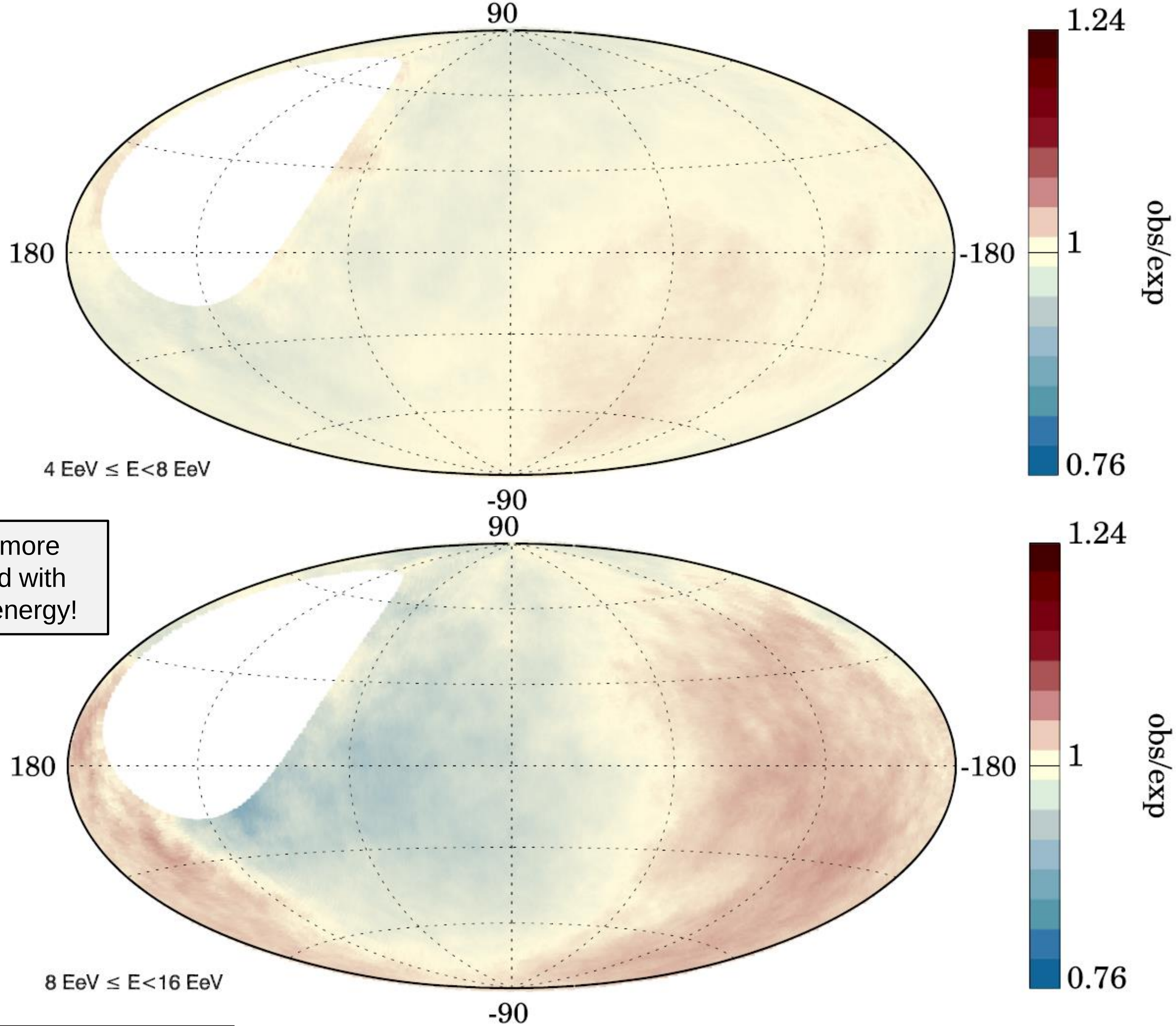

Excesses more pronounced with increasing energy!

Maps are in galactic coordinates

Cosmic ray excess maps

Anisotropy studies

Cosmic ray excess maps

Anisotropy studies

Cosmic ray excess maps

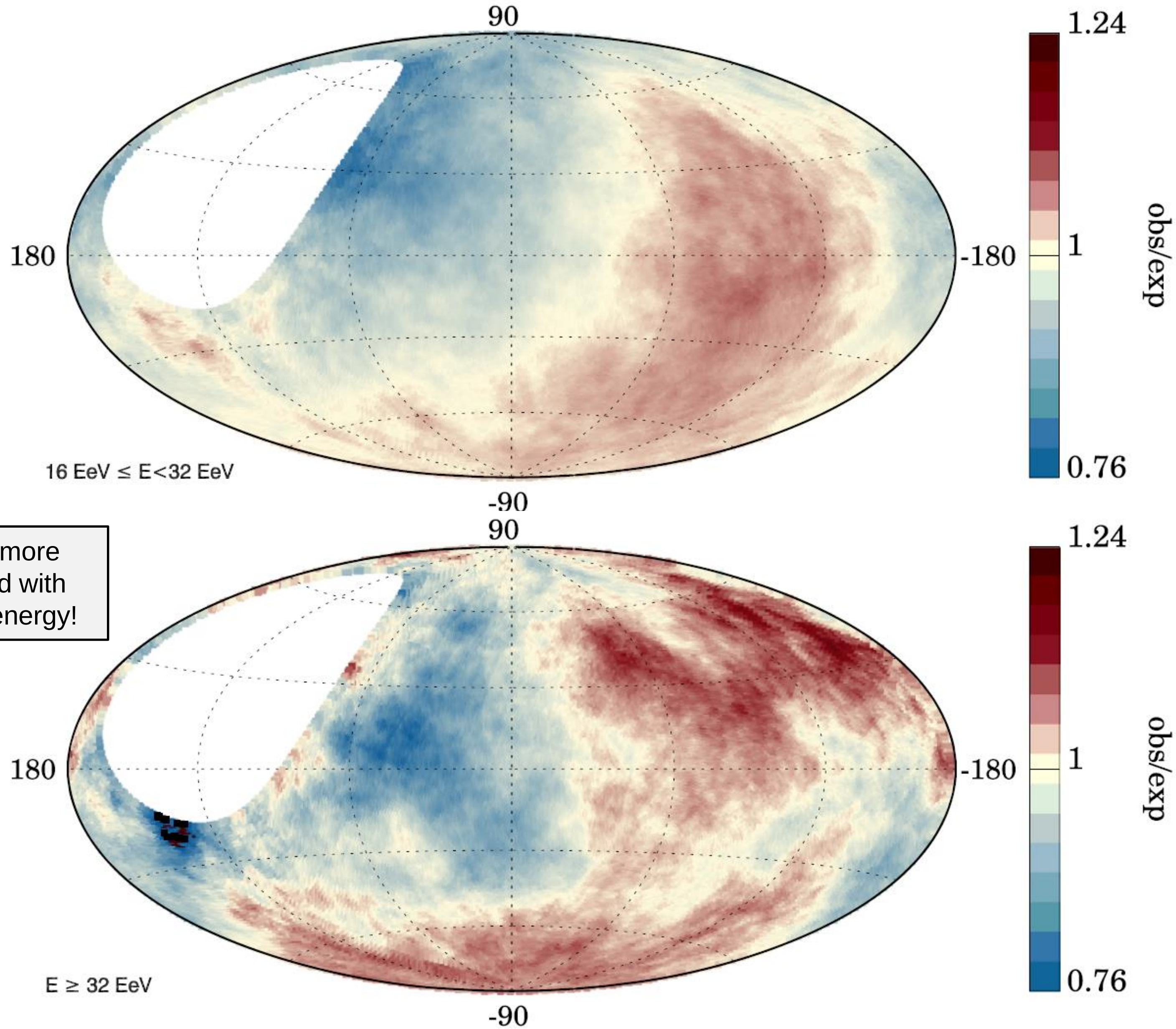

Excesses more pronounced with increasing energy!

Maps are in galactic coordinates

Intermediate-scale anisotropy

Intermediate-scale anisotropy: Search for modulation of arrival directions above 20 EeV

Auger data between January 1st 2004 and April 30th 2017, exposure 89,720 km^2 sr yr

Search for a correlation between arrival directions and strong nearby sources: Active Galactic Nuclei (AGN), Starburst Galaxies (SBG)

Catalogs used: 2FHL (Fermi-LAT), Swift-BAT, 2MRS (2MASS redshift survey)

UHECR fluxes have been corrected for attenuation

SBGs	l (°)	b (°)	Distance[a] (Mpc)	Flux Weight (%)	Attenuated Weight: A/B/C (%)	% Contribution[b]: A/B/C (%)
NGC 253	97.4	−88	2.7	13.6	20.7/18.0/16.6	35.9/32.2/30.2
M82	141.4	40.6	3.6	18.6	24.0/22.3/21.4	0.2/0.1/0.1
NGC 4945	305.3	13.3	4	16	19.2/18.3/17.9	39.0/38.4/38.3
M83	314.6	32	4	6.3	7.6/7.2/7.1	13.1/12.9/12.9
NGC 1068	172.1	−51.9	17.9	12.1	5.6/7.9/9.0	6.4/9.4/10.9
γAGNs						
Cen A Core	309.6	19.4	3.7	0.8	60.5/14.6/40.4	86.8/56.3/71.5
M87	283.7	74.5	18.5	1	15.3/7.1/29.5	9.7/12.1/23.1
NGC 1275	150.6	−13.3	76	2.2	6.6/6.1/7.5	0.7/1.6/1.0
Mkn 421	179.8	65	136	54	11.4/48.3/14.7	1.8/19.1/2.8

Notes.
[a] A standard, flat ΛCDM model ($h_0 = 0.7$, $\Omega_M = 0.3$) is assumed. The distances of the SBGs are based on Ackermann et al. (2012), accounting for a small difference in h_0. The distances of the γAGNs are based on their redshifts, except for the nearby Cen A (Tully et al. 2013).
[b] % contributions account for the directional exposure of the array.

Maximum likelihood analysis

Correlation performed with unbinned maximum likelihood analysis

Test statistic (TS) is the likelihood ratio test between two hypothesis:
UHECR sky model and an isotropic model

Two variables: anisotropic fraction (fraction of events due to sources) and search radius (RMS angular separation from sources)

Maximum TS (AGNs):
E > 60 EeV,
$\mathbf{2.7\sigma}$ **deviation**,
$7^{+4}_{-2}{}^{\circ}$ search radius,
$7 \pm 4\%$ anisotropic fraction

Maximum TS (SBGs):
E > 39 EeV,
$\mathbf{4.0\sigma}$ **deviation**,
$13^{+4}_{-3}{}^{\circ}$ search radius,
$10 \pm 4\%$ anisotropic fraction

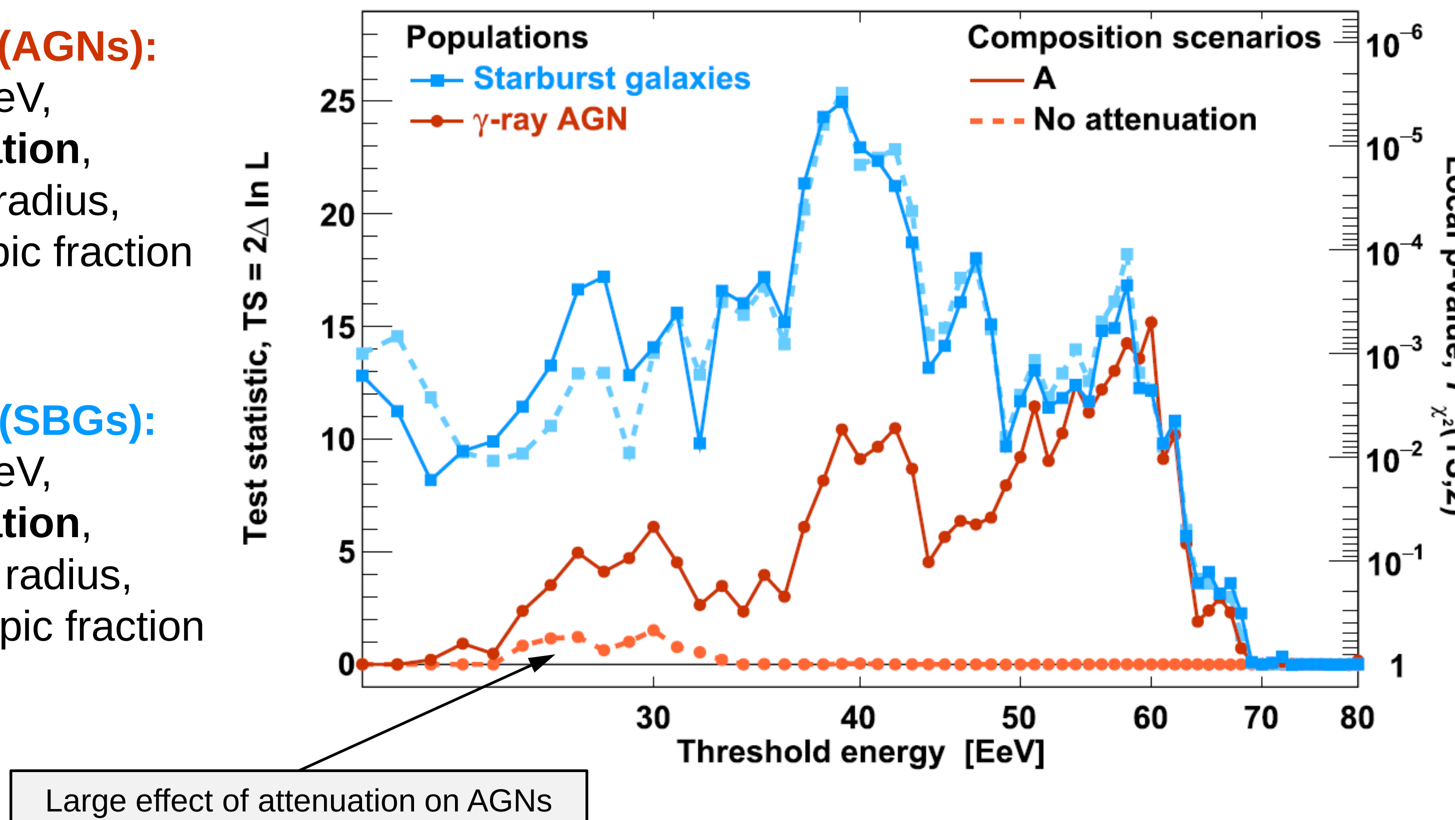

Maximum likelihood analysis

Correlation performed with unbinned maximum likelihood analysis

Test statistic (TS) is the likelihood ratio test between two hypothesis:
UHECR sky model and an isotropic model

Two variables: anisotropic fraction (fraction of events due to sources) and search radius (RMS angular separation from sources)

Maximum TS (Swift-BAT):
E > 39 EeV,
$\mathbf{3.2\sigma}$ **deviation**,
$12^{+6}_{-4}{}^{\circ}$ search radius,
$7^{+4}_{-3}\%$ anisotropic fraction

Maximum TS (2MRS):
E > 38 EeV,
$\mathbf{2.7\sigma}$ **deviation**,
$13^{+7}_{-4}{}^{\circ}$ search radius,
$16^{+8}_{-7}\%$ anisotropic fraction

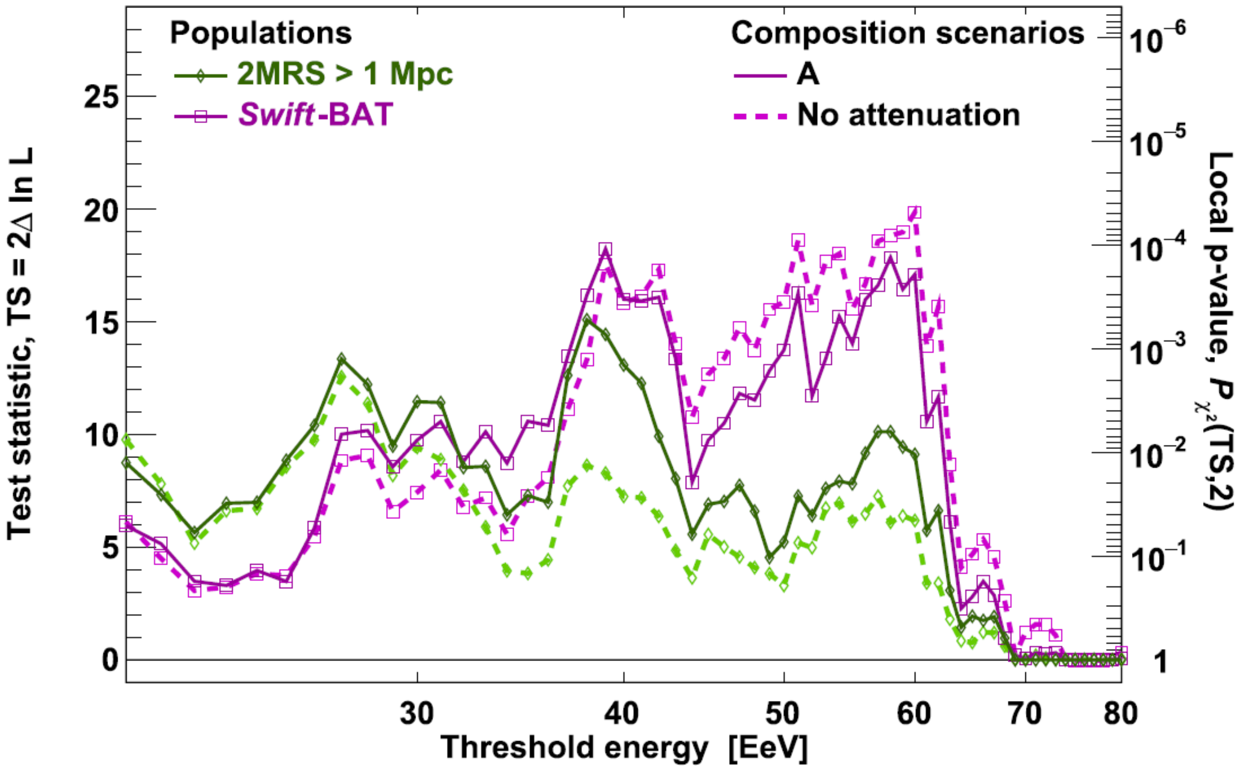

Cosmic ray excess maps

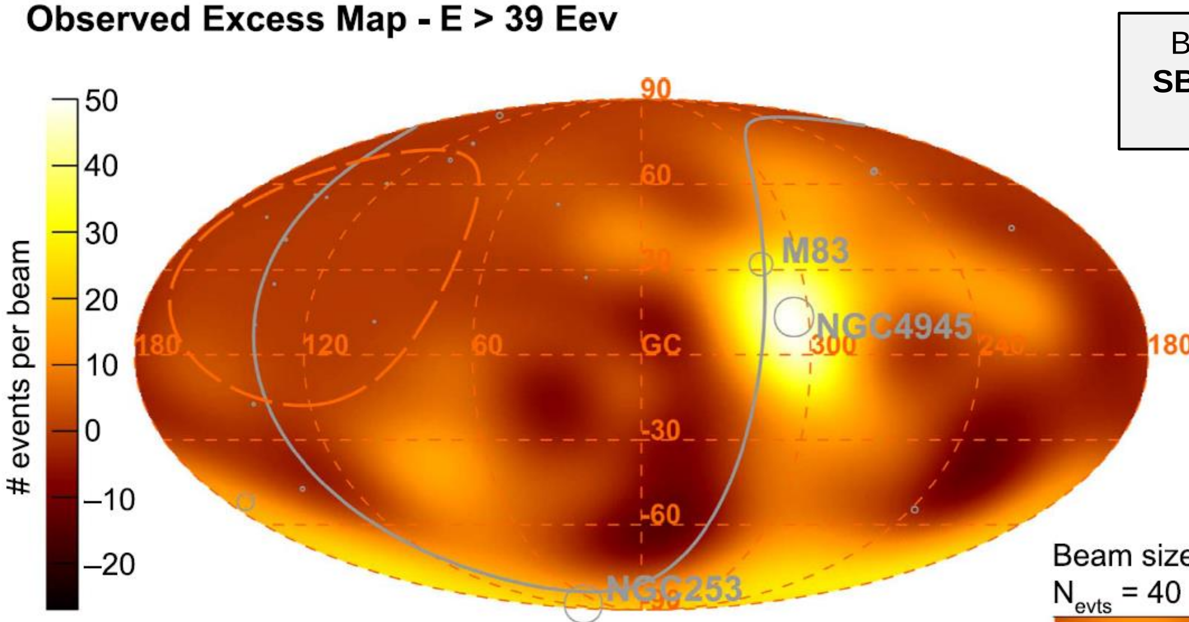

Brightest sources are **SBGs** (M83, NGC4945, NGC253)!

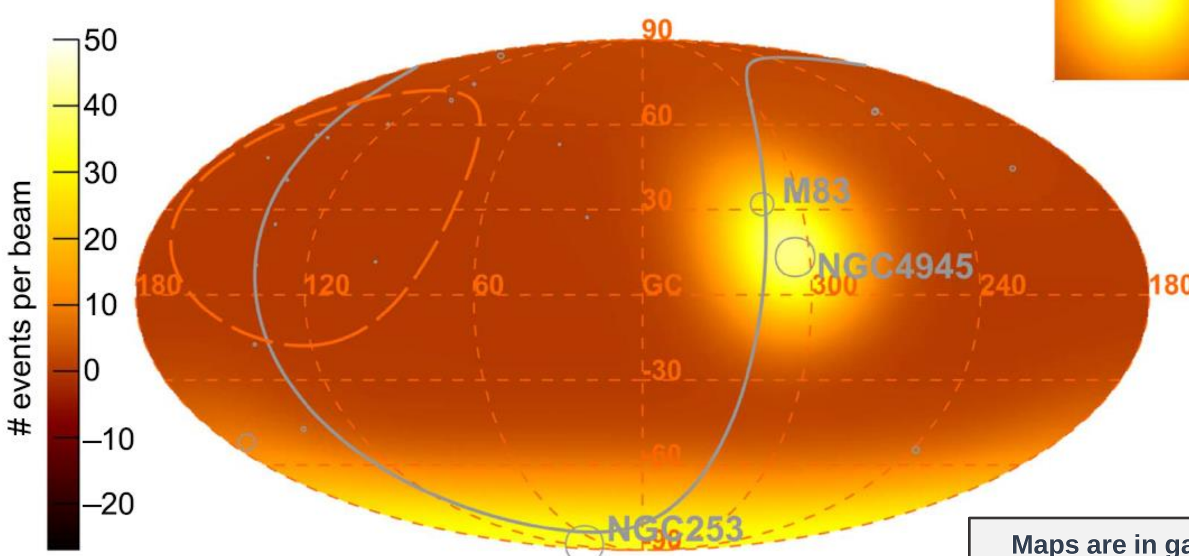

Maps are in galactic coordinates

Cosmic ray excess maps

Brightest sources are **AGNs** (Centaurus A)!

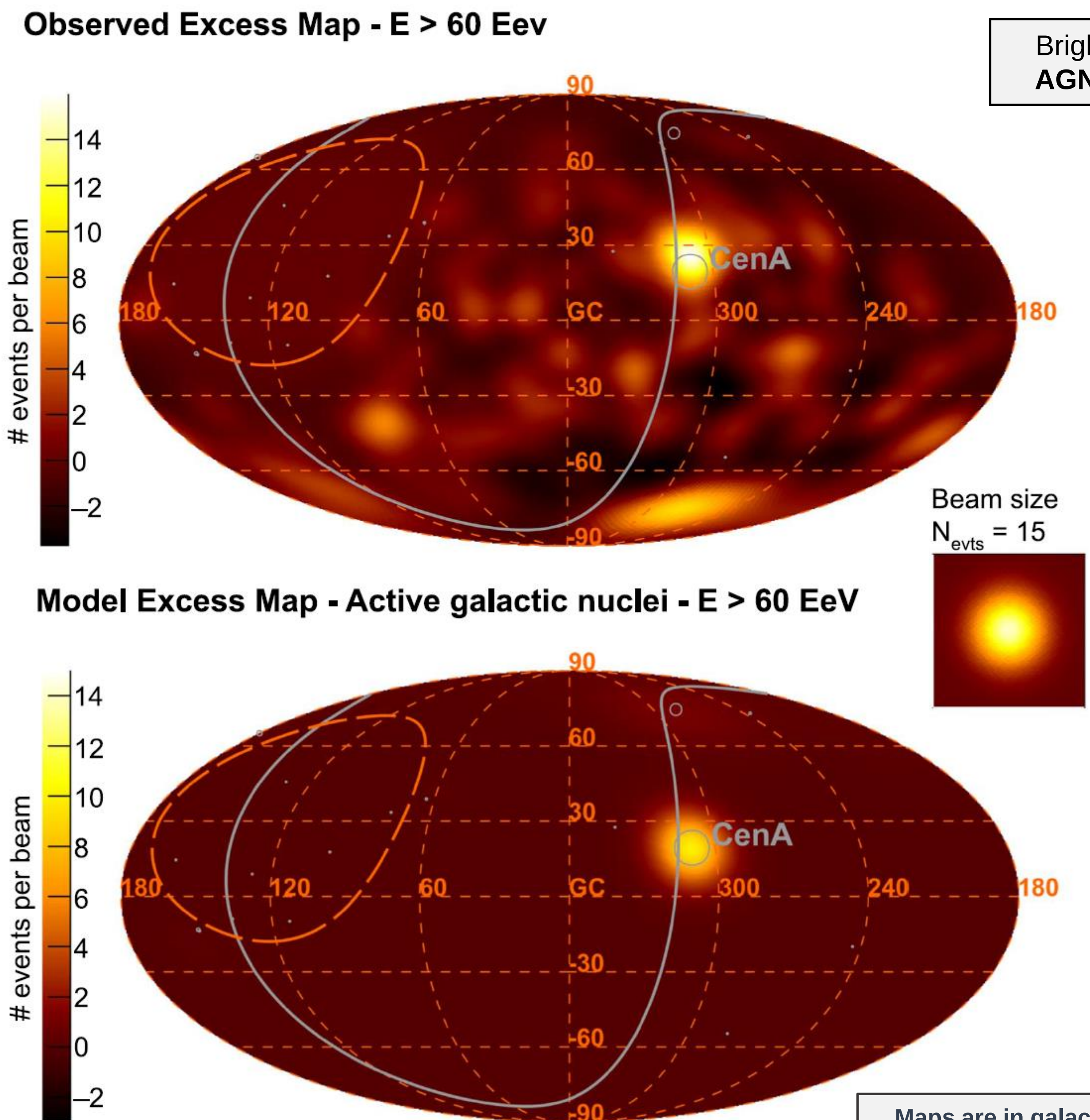

Maps are in galactic coordinates

Conclusions

Large-scale anisotropy

Largest dipolar modulation at E ≥ 8 EeV, $(l, b) = (233°, -13°)$
Located ~125° away from galactic center → **Extragalactic origin!**

Quadrupolar contributions are not statistically significant

Intermediate-scale anisotropy

Isotropy of UHECR is disfavored with a $\mathbf{4.0\sigma}$ **confidence**
Best matched by a model with 10% of cosmic ray events clustered around bright nearby SBGs

Combined with analysis from the Telescope Array (TA), the full-sky data will soon be available

---

Uncertainties on the galactic magnetic field model and UHECR mass composition:

- Make it difficult to infer the dipole structure outside our galaxy
- Yield larger deviations from source direction (larger search radius)

Multimessenger studies

Multimessenger: In addition to UHECR, observatory also sensitive to UHE neutrinos and photons

Diffuse candidates: Searching for candidates diffuse neutrino and photon fluxes

Point source candidates: Performing targeted searches with correlated point sources

Main difficulties come from low statistics at the highest energies

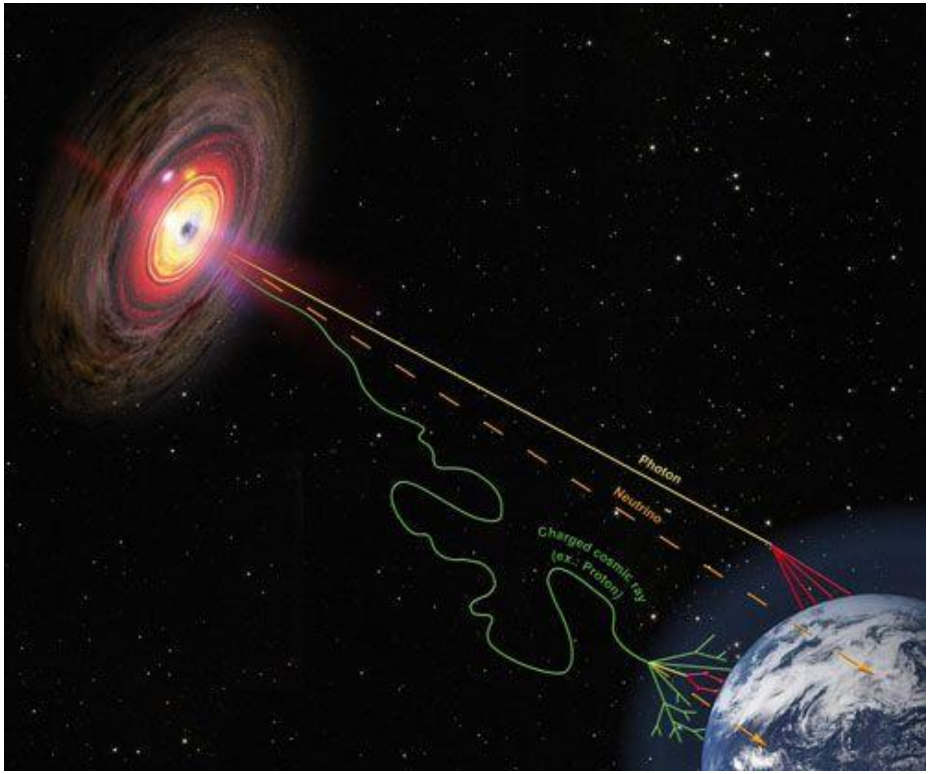

Search for neutrinos

Neutrinos are neutral and interact weakly → perfect for uncovering sources

Produced in sources (astrophysical) or during interaction with CMB photons (cosmogenic)

At Pierre Auger Observatory, observed as highly inclined events:
down-going low $(60° < \theta < 75°)$
down-going high $(75° < \theta < 90°)$
Earth-skimming $(90° < \theta < 95°)$

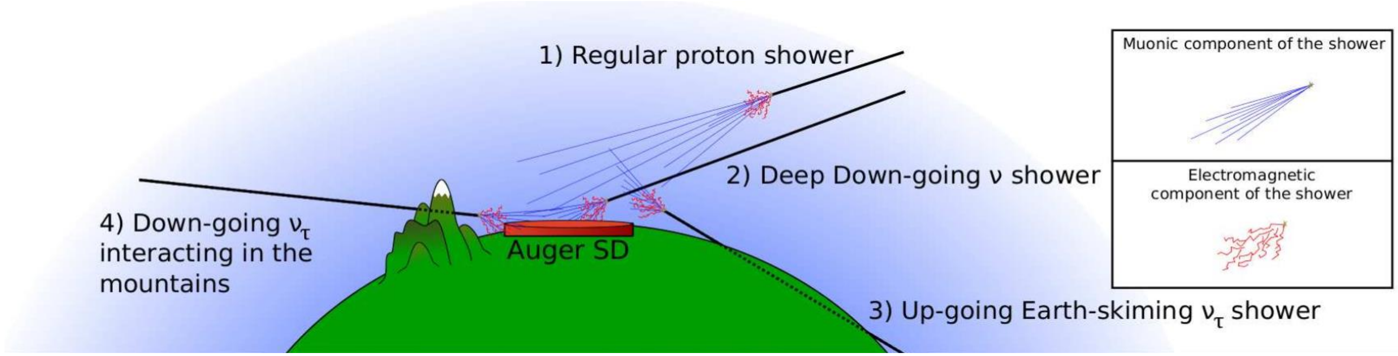

Discrimination from normal CR showers based off of the EAS age

Perform a Fisher analysis to select the cut for candidates

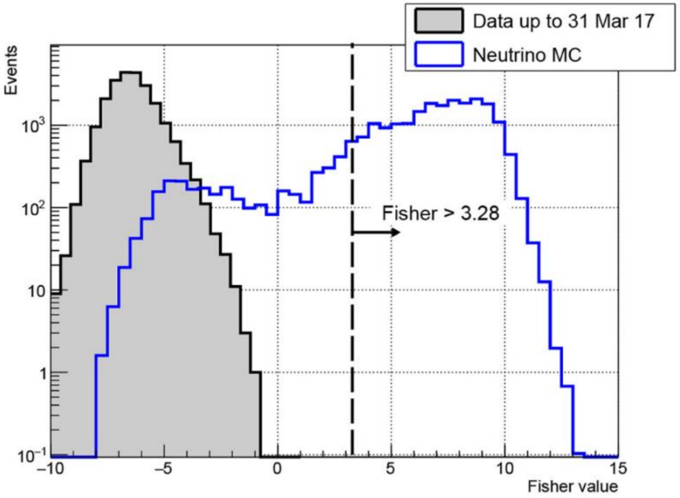

Diffuse neutrino limits

Search for diffuse UHE neutrinos at $-85° < \delta < 60°$ → No neutrino candidates found!

Set a stringent upper limit that excludes some neutrino production models

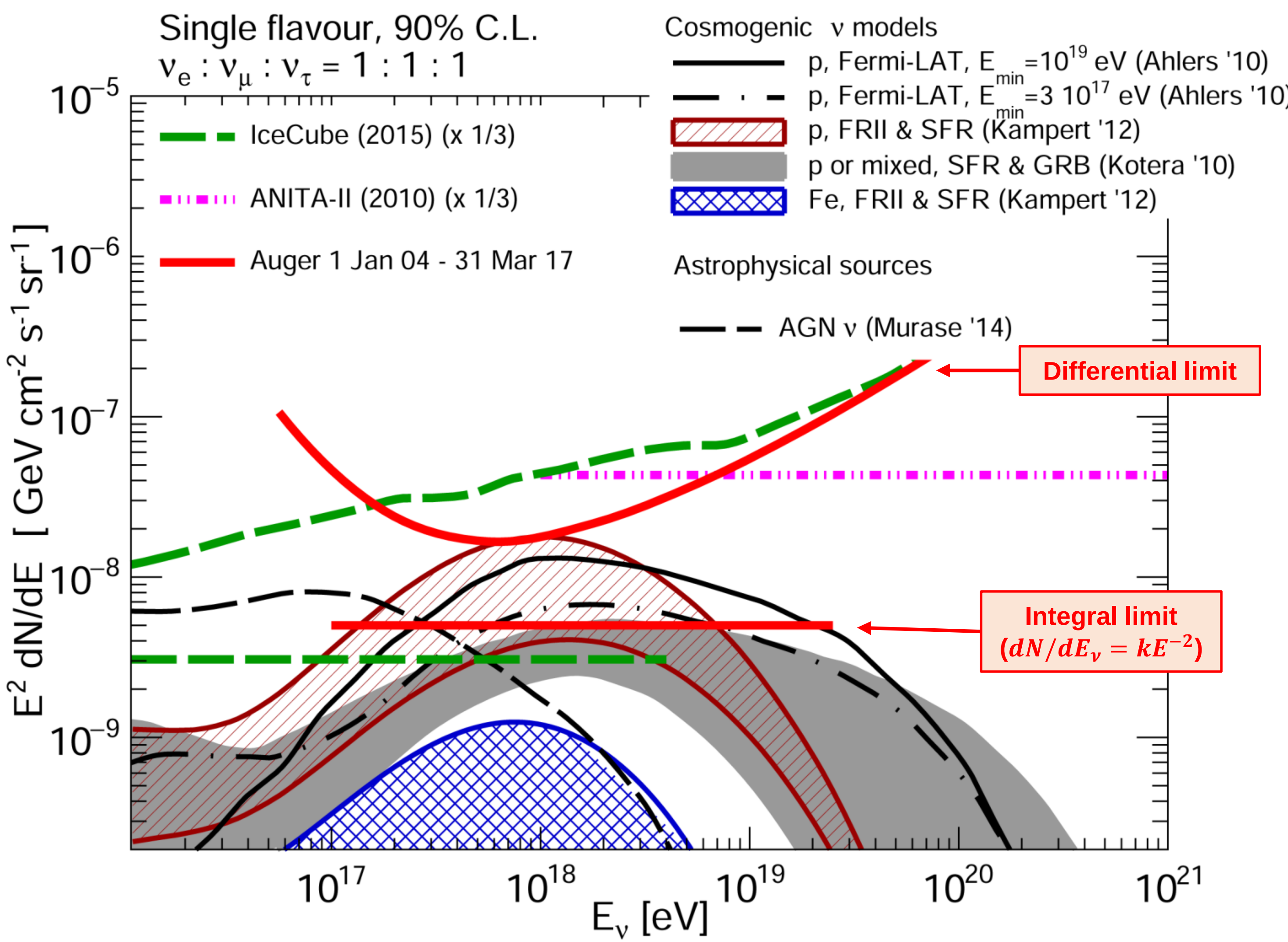

Point source neutrino limits

Since no candidates have been found (up to March 31st 2017), limits are also set for point sources

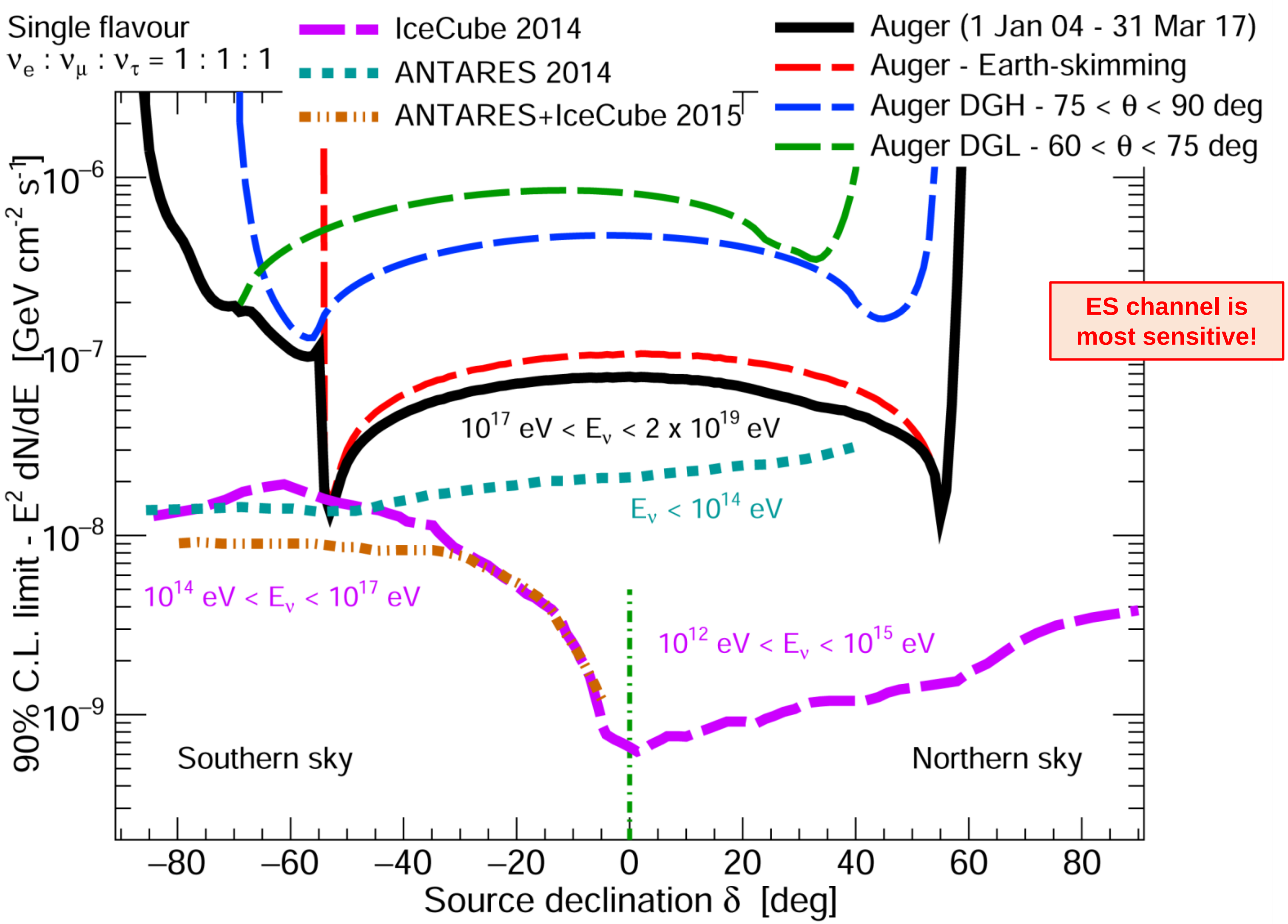

ES channel is most sensitive!

Gravitational wave events

Neutrinos are early alerts for astrophysical processes → dedicated searches during gravitational wave (GW) events

Correlated search with a **±500 s** window (prompt GRB phase) and a **+1 day** window (GRB afterglows)

Most promising event **GW170817** appeared to be in the Earth-skimming channel (most sensitive to neutrinos) → No candidates found!

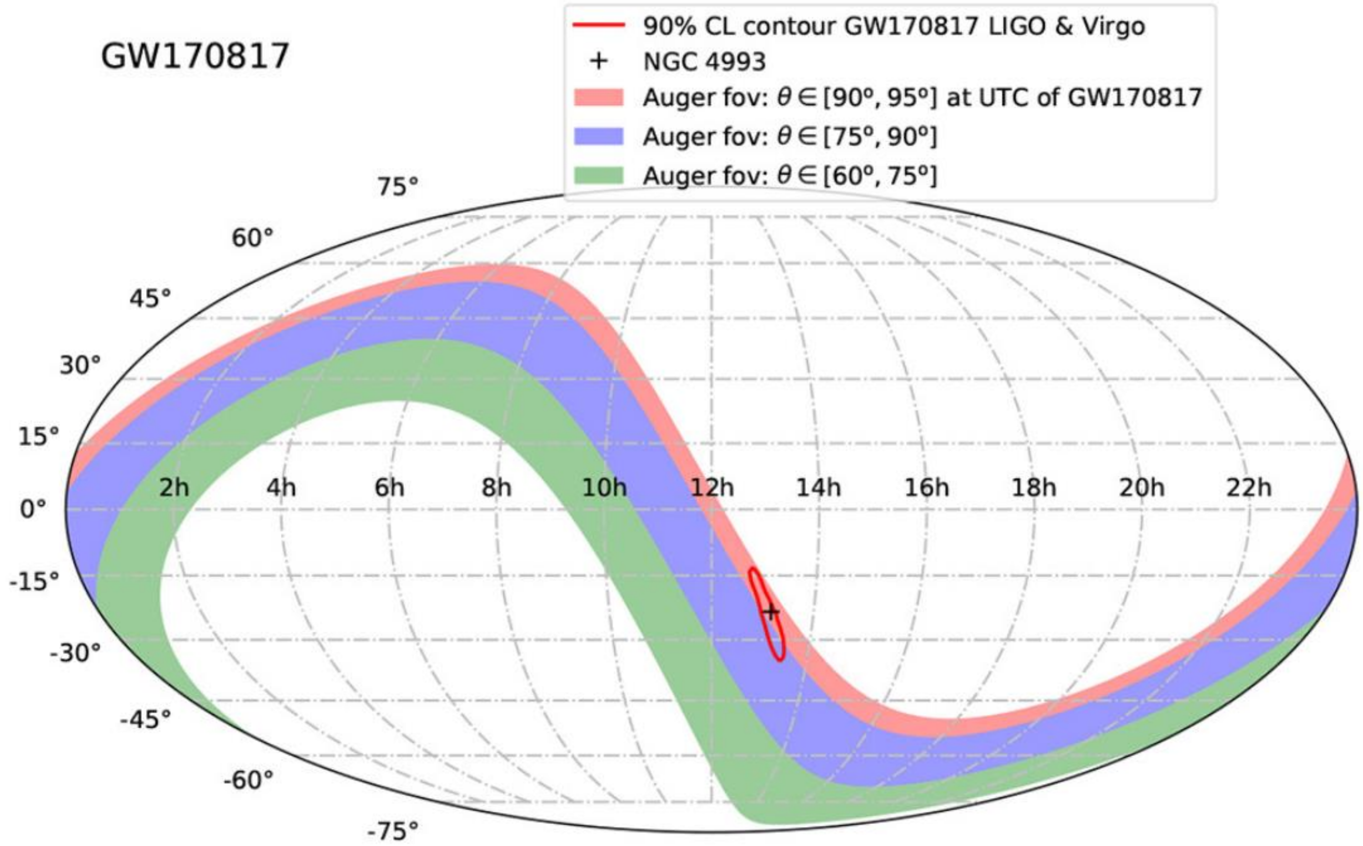

Gravitational wave events

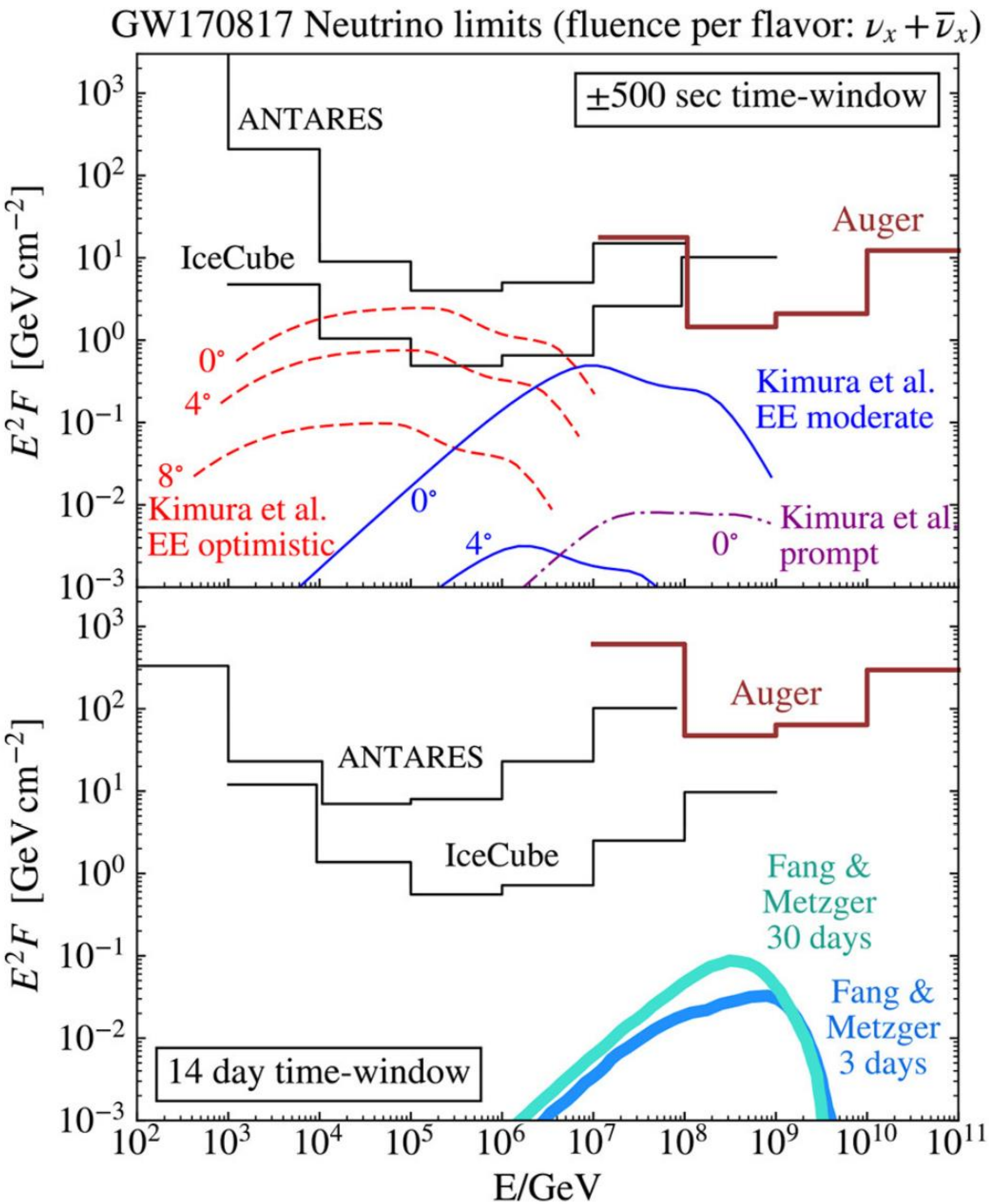

Non-detection sets upper limits for neutrinos produced in neutron star mergers

Search for photons

Photons are neutral and are good candidates for point source searches

Produced in GZK processes, interaction with extragalactic background light (EBL) and top-down models predicting dark matter

Attenuation length at EeV energies is ~4.5 Mpc → detection from nearby sources (up to Centaurus A)

Perform a multivariate analysis using Boosted decision trees (BDT) to discriminate from normal CR showers

Selected cut gives a very small contamination with background $(0.04 - 0.14\%)$

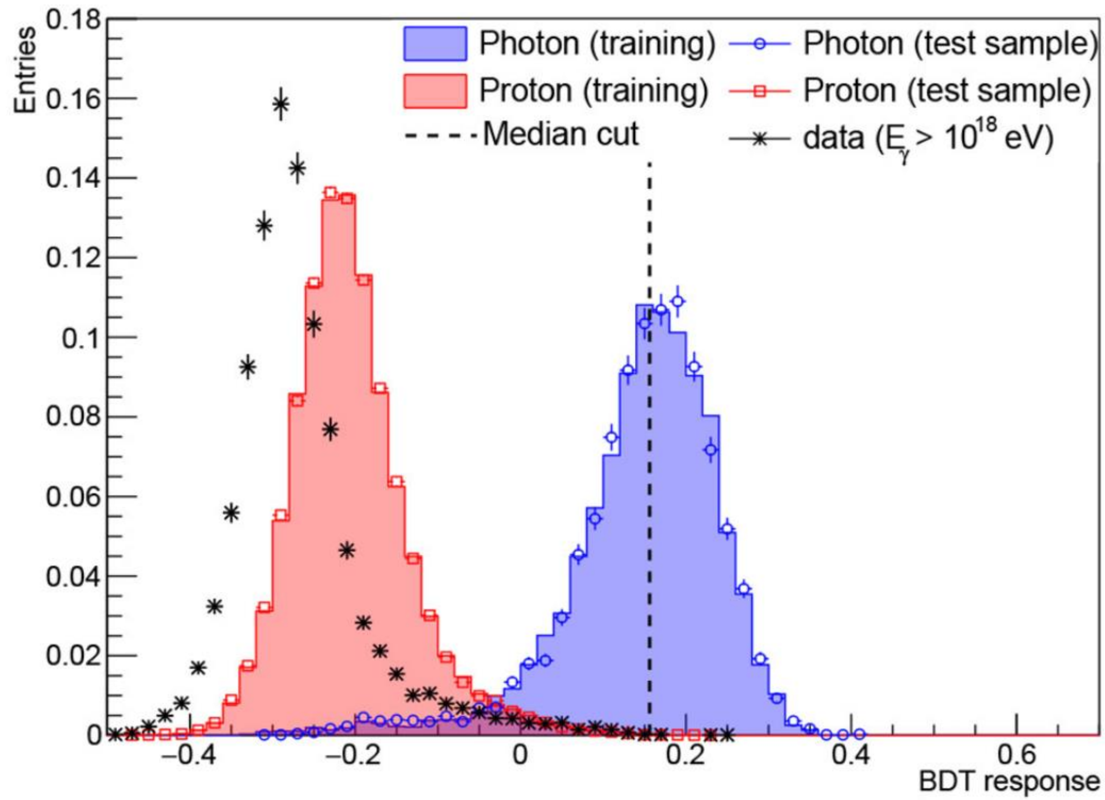

Diffuse photon limits

Search for diffuse UHE photons → 8 candidates, which have to be analysed further

Set a stringent upper limit that excludes some photon production models

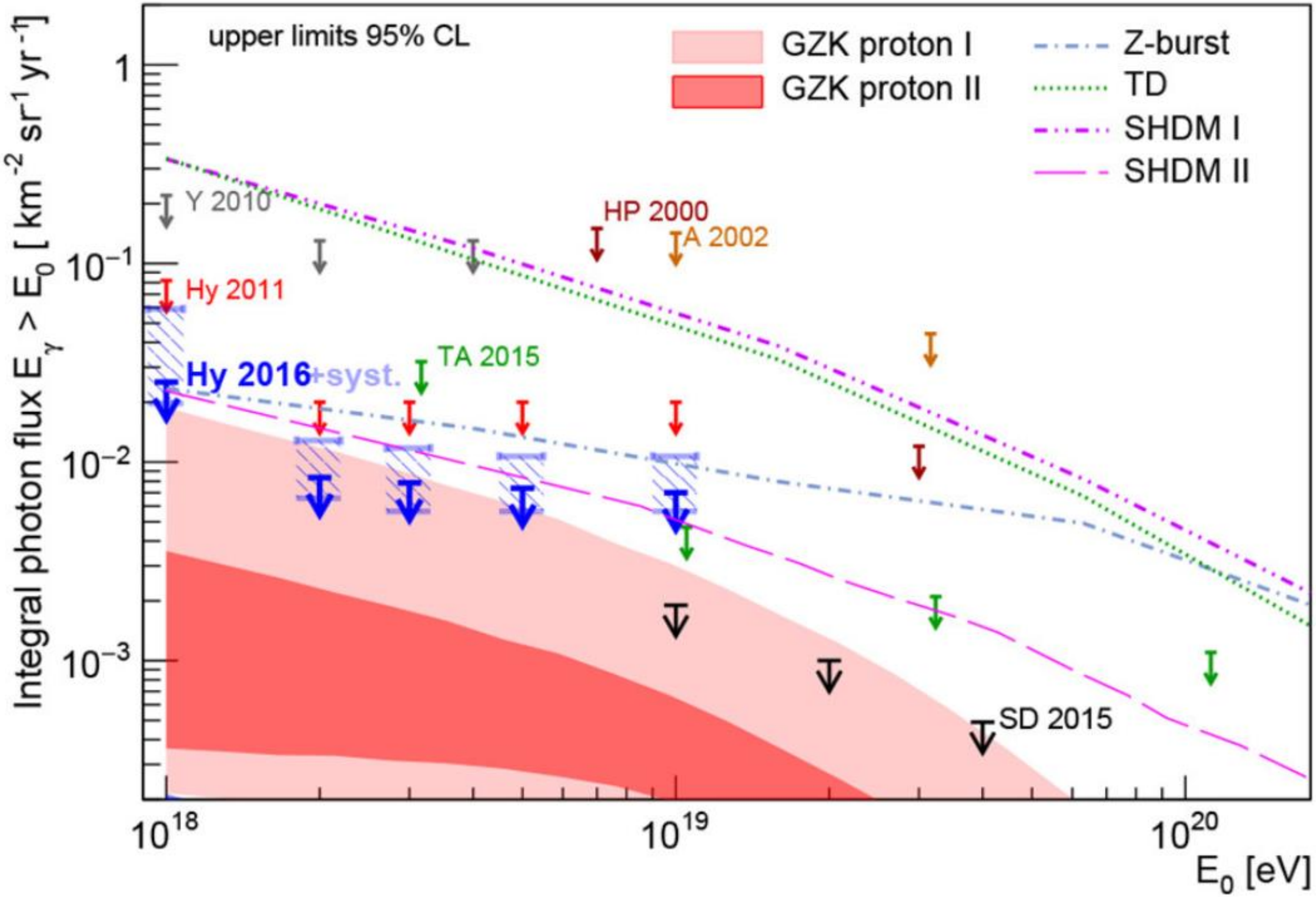

Point source photon limits (GC)

Specific interest for point sources is the galactic center (GC) → H.E.S.S. measurements have uncovered a PeVatron

No candidates found with additional correlated searches → UHE photons might have an extragalactic origin, might be from transient sources or sources have misaligned jets

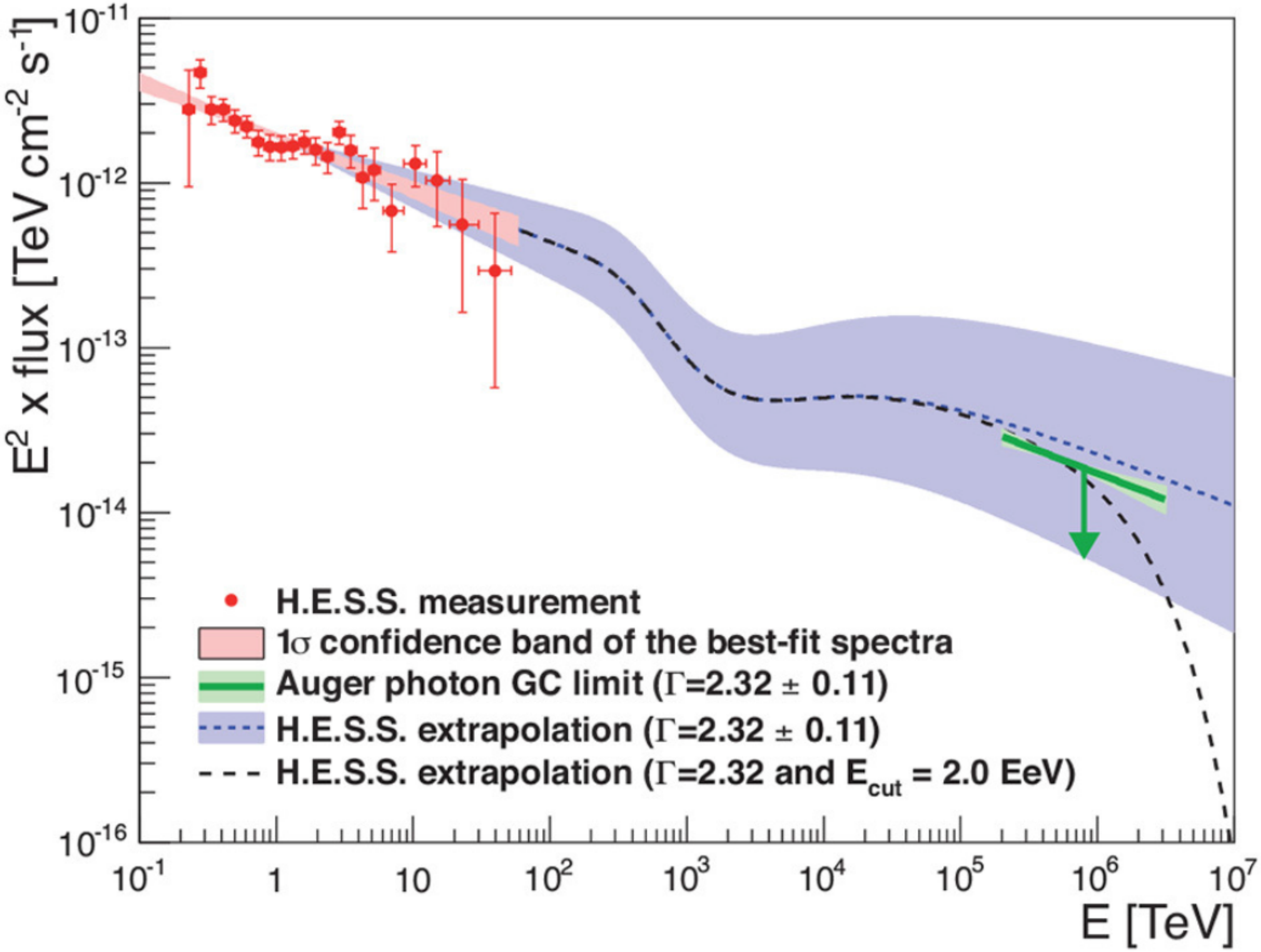

Conclusions

UHE neutrinos

Search for diffuse neutrinos and point source neutrinos have not uncovered any candidates

No neutrinos correlated with GW events have been found yet

Sets stringent upper limits for detection, excludes some models of UHE neutrino production

---

UHE photons

Search for diffuse photons have uncovered 8 candidates, which will be investigated further

No point sources for photons have been found yet

Sets stringent upper limits for detection and excludes some top-down models of UHE photon production

Gamma-ray sources might not have enough energy to reach the threshold of the Pierre Auger Observatory or their spectrum is softer

---

Alert system being prepared to automatically alert other observatories/telescopes → Astrophysical Multi-messenger Observatory Network (AMON)

SD upgrade adds scintillators on existing SDs (better estimation of EM/muon content)

Thank you for your attention!

References

1. A. Aab *et al.*, *Large-scale Cosmic-Ray Anisotropies above 4 EeV Measured by the Pierre Auger Observatory*, doi:10.3847/1538-4357/aae689.
2. A. Aab *et al.*, *An Indication of Anisotropy in Arrival Directions of Ultra-high-energy Cosmic Rays through Comparison to the Flux Pattern of Extragalactic Gamma-Ray Sources*, doi:10.3847/2041-8213/aaa66d.
3. A. Aab *et al.*, *Improved limit to the diffuse flux of ultrahigh energy neutrinos from the Pierre Auger Observatory*, doi:10.1103/PhysRevD.91.092008.
4. ANTARES, IceCube, Pierre Auger, LIGO and Virgo Collaborations, *Search for High-energy Neutrinos from Binary Neutron Star Merger GW170817 with ANTARES, IceCube, and the Pierre Auger Observatory*, doi:10.3847/2041-8213/aa9aed.
5. A. Aab *et al.*, *Search for photons with energies above 10^{18} eV using the hybrid detector of the Pierre Auger Observatory*, doi:10.1088/1475-7516/2017/04/009.
6. A. Aab *et al.*, A targeted search for point sources of EeV photons with the Pierre Auger Observatory, doi:10.3847/2041-8213/aa61a5.
7. K.-H. Kampert, M. A. Mostafa, E. Zas and The Pierre Auger Collaboration, *Multi-messenger Physics With the Pierre Auger Observatory*, doi:10.3389/fspas.2019.00024.

Backup slides

GZK effect

Graisen-Zatsepin-Kuzmin effect: Abrupt drop at the highest energies, scattering of protons and neutrons on CMB photons

$$p + \gamma_{CMB} \longrightarrow n + \pi^+$$

$$n + \gamma_{CMB} \longrightarrow p + \pi^-$$

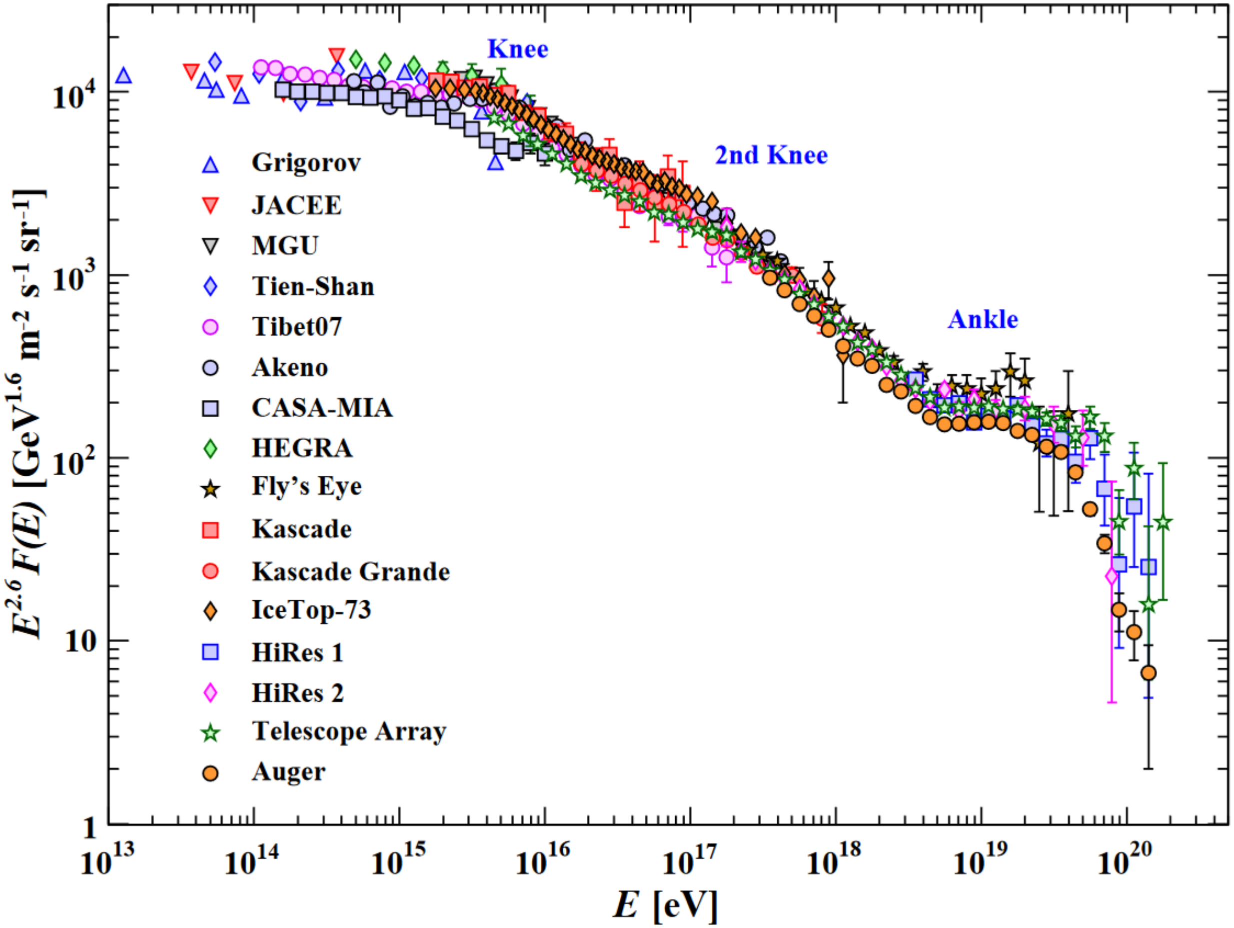

Extensive air shower

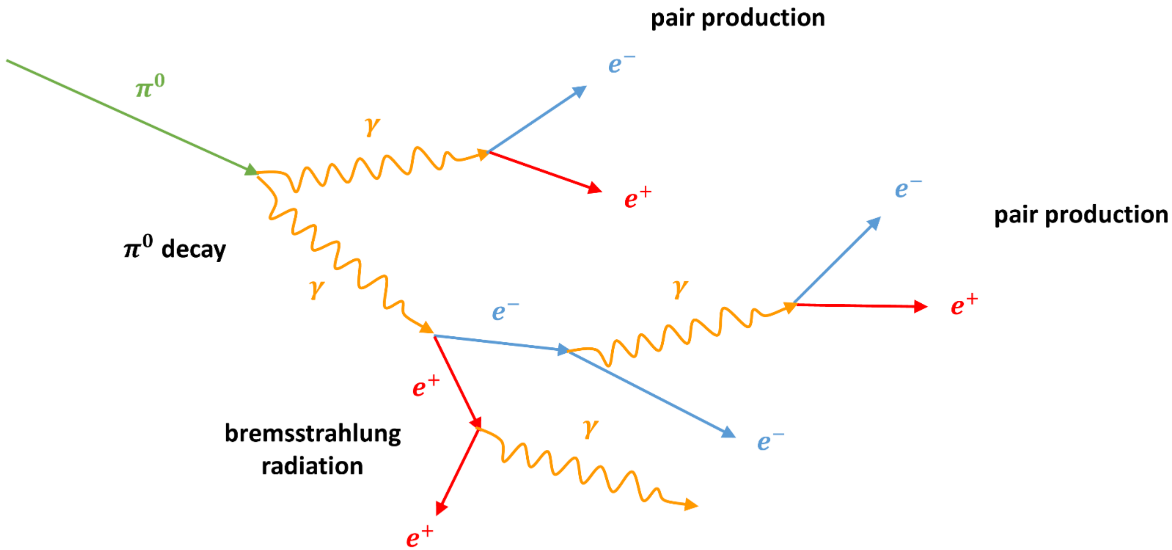

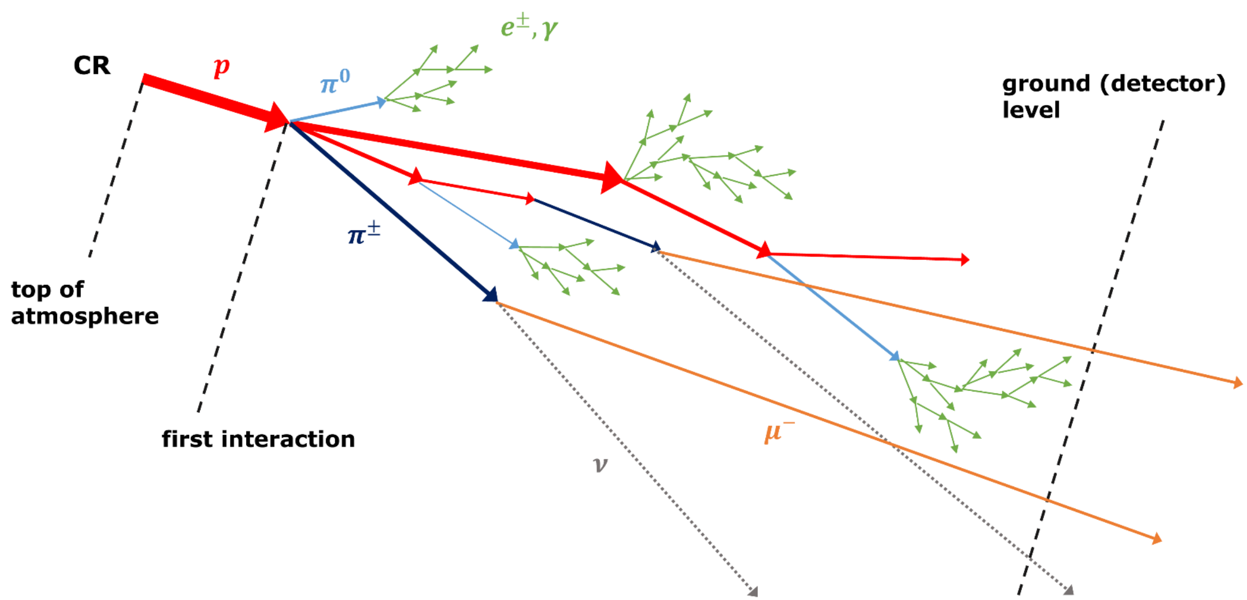

FD telescope

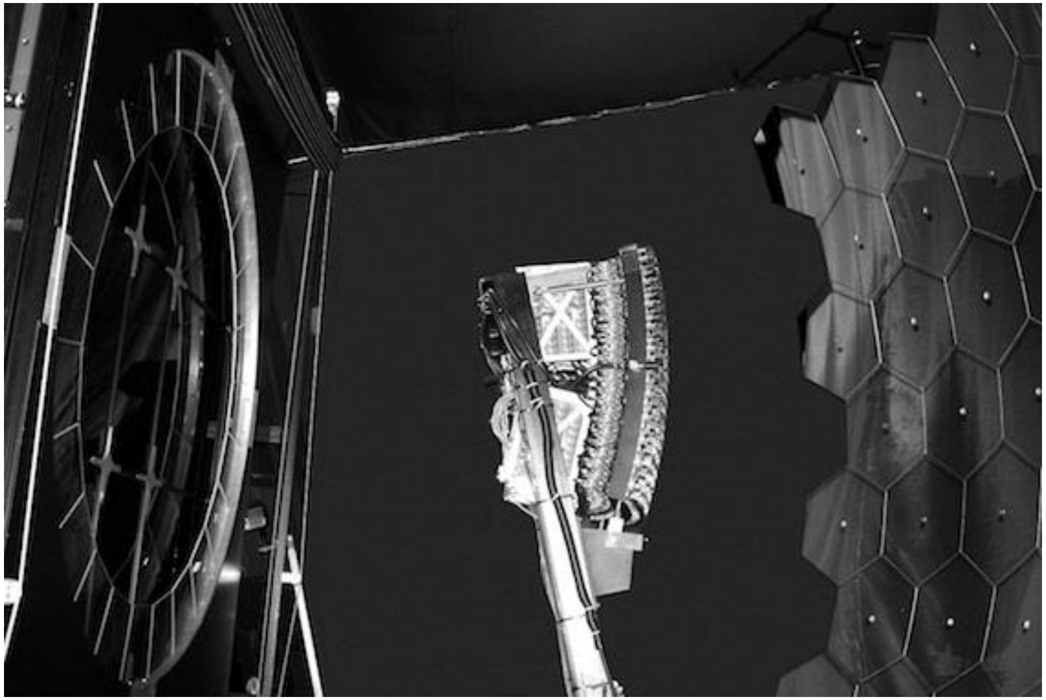

Hybrid detection

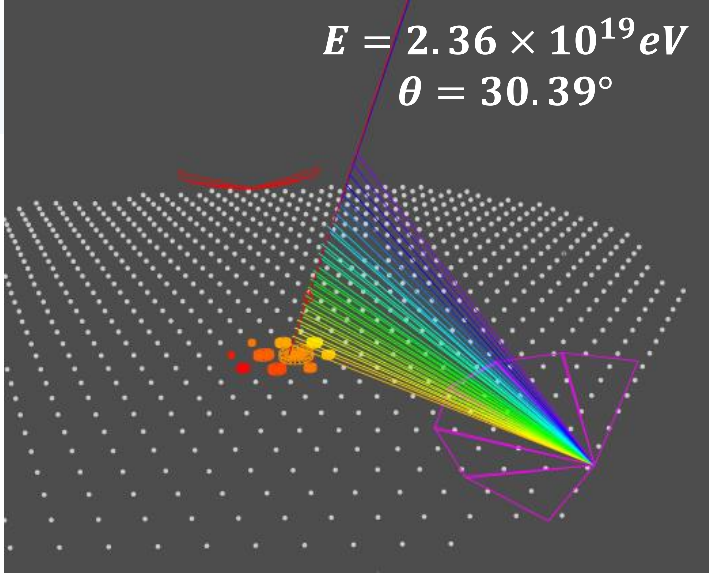

Hybrid event: Event observed with SD and FD

Event reconstruction gives information on primary UHECR, development of EAS and its footprint on the ground

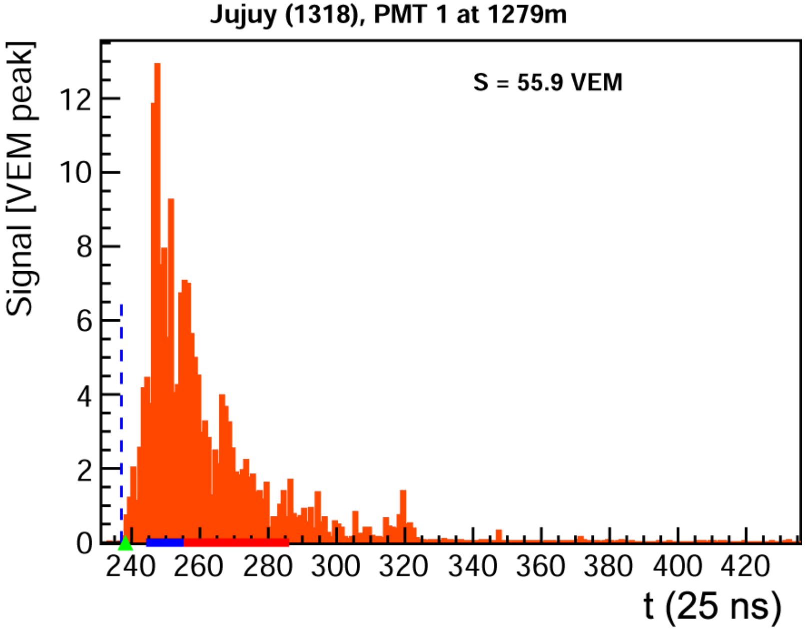

SD signal

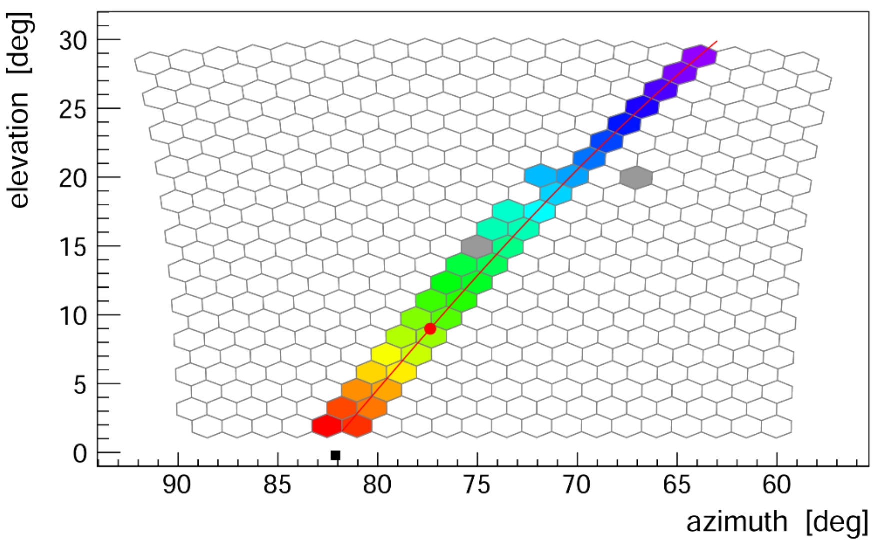

FD signal

Large-scale anisotropy

Large-scale anisotropy: Search for modulation of arrival directions above 4 EeV

Auger data between January 1st 2004 and August 31st 2016, exposure 76,800 km^2 sr yr

Perform a Fourier analysis on RA (α) and azimuth (ϕ) → gain information on structure and estimate UHECR flux excess

$$a_k^x = 2\frac{\sum_{i=1}^N w_i \cos(k\,x_i)}{\sum_{i=1}^N w_i}$$

$$b_k^x = 2\frac{\sum_{i=1}^N w_i \sin(k\,x_i)}{\sum_{i=1}^N w_i}$$

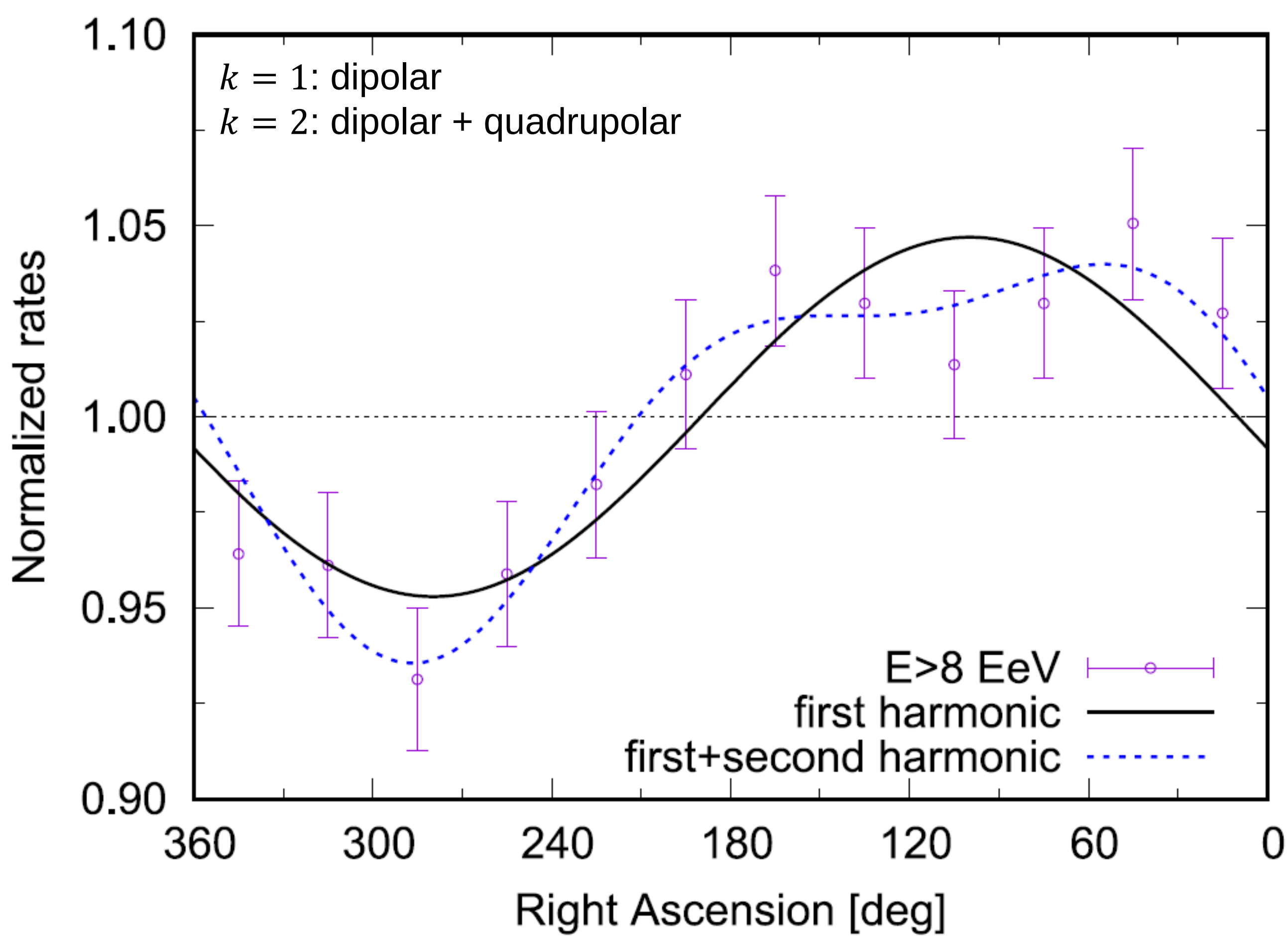

Significant East/West dipolar contribution in RA analysis (~100°)!

Dipolar structure

Highest energy bin split to three bins in order to get the dipolar amplitude dependence

Dipole $\boldsymbol{d} = (d_\perp, d_z)$ is calculated from RA and azimuth:

$$d_z \simeq \frac{b_1^\phi}{\cos l_{obs} \langle \sin\theta \rangle} \qquad d_\perp \simeq \frac{\sqrt{(a_1^\alpha)^2 + (b_1^\alpha)^2}}{\langle \cos\delta \rangle}$$

$$\alpha_d = \arctan\left(\frac{b_1^\alpha}{a_1^\alpha}\right)$$

$$\delta_d = \arctan\left(\frac{d_z}{d_\perp}\right)$$

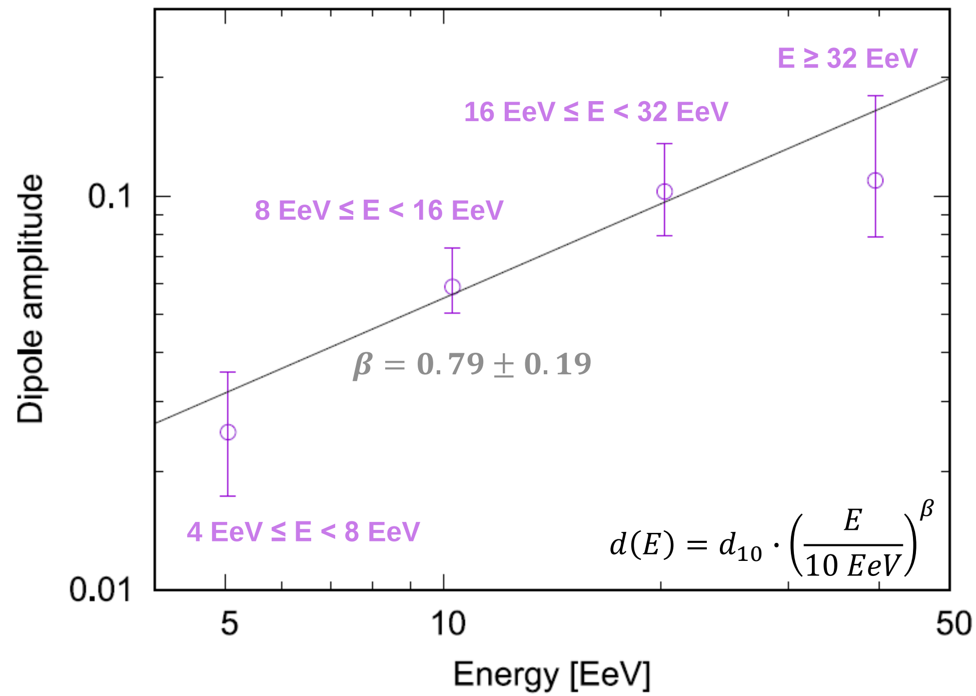

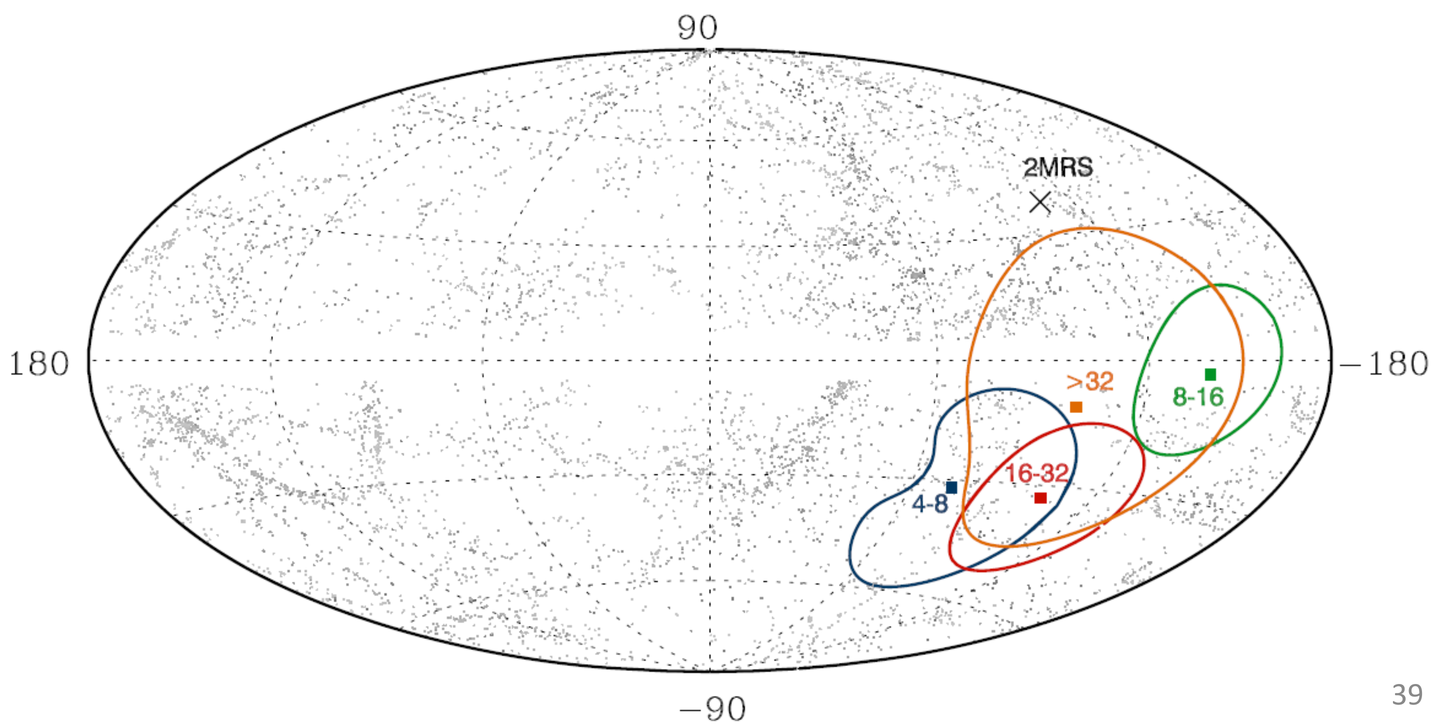

Shower age from SD signal

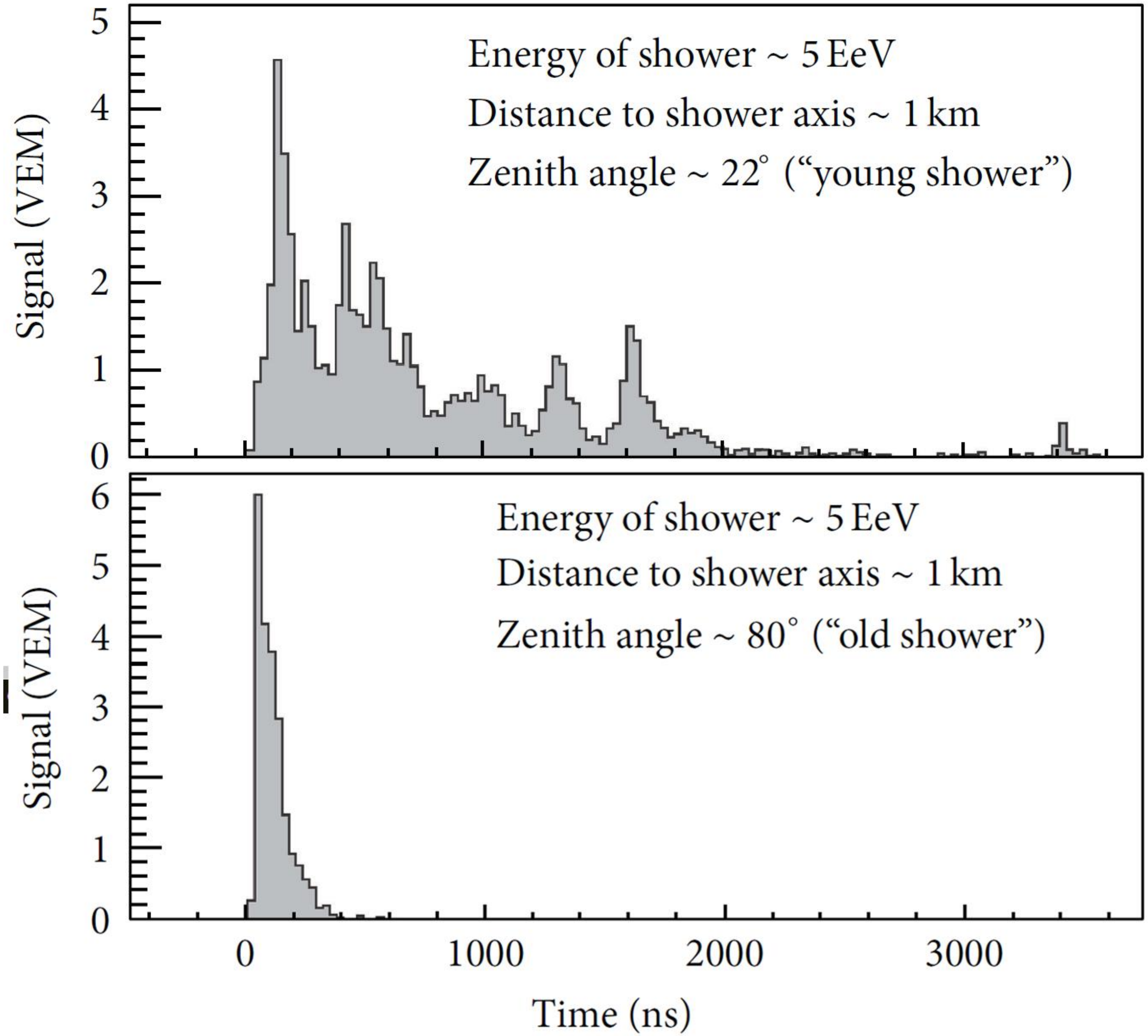

Neutrino interactions